

RESEARCH ARTICLE | DECEMBER 17 2025

Connections between Richardson–Gaudin states, perfect-pairing, and pair coupled-cluster theory

Paul A. Johnson  ; Charles-Émile Fecteau  ; Samuel Nadeau  ; Mauricio Rodríguez-Mayorga  ; Pierre-François Loos 



J. Chem. Phys. 163, 234115 (2025)
<https://doi.org/10.1063/5.0305612>



Articles You May Be Interested In

Transition density matrices of Richardson–Gaudin states

J. Chem. Phys. (March 2021)

Near-exact treatment of seniority-zero ground and excited states with a Richardson–Gaudin mean-field

J. Chem. Phys. (May 2022)

Pair extended coupled cluster doubles

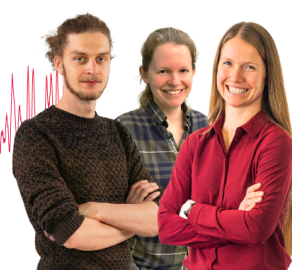
J. Chem. Phys. (June 2015)

Webinar From Noise to Knowledge

May 13th – Register now



Universität
Konstanz



Connections between Richardson–Gaudin states, perfect-pairing, and pair coupled-cluster theory

Cite as: J. Chem. Phys. 163, 234115 (2025); doi: 10.1063/5.0305612

Submitted: 7 October 2025 • Accepted: 1 December 2025 •

Published Online: 17 December 2025



View Online



Export Citation



CrossMark

Paul A. Johnson,^{1,a)} Charles-Émile Fecteau,¹ Samuel Nadeau,¹ Mauricio Rodríguez-Mayorga,² and Pierre-François Loos²

AFFILIATIONS

¹ Département de Chimie, Université Laval, Québec, Québec G1V 0A6, Canada

² Laboratoire de Chimie et Physique Quantiques (UMR 5626), Université de Toulouse, CNRS, Toulouse, France

^{a)} Author to whom correspondence should be addressed: paul.johnson@chm.ulaval.ca

ABSTRACT

Slater determinants underpin most electronic structure methods, but orbital-based approaches often struggle to describe strong correlation efficiently. Geminal-based theories, by contrast, naturally capture static correlation in bond-breaking and multi-reference problems, though at the expense of implementation complexity and limited treatment of dynamic effects. In this work, we examine the interplay between orbital and geminal frameworks, focusing on perfect-pairing (PP) wavefunctions and their relation to pair coupled-cluster doubles (pCCD) and Richardson–Gaudin states. We show that PP arises as an eigenvector of a simplified, reduced Bardeen–Cooper–Schrieffer Hamiltonian expressed in bonding/antibonding orbital pairs, with the complementary eigenvectors enabling a systematic treatment of weak correlation. Second-order Epstein–Nesbet perturbation theory on top of PP is found to yield energies nearly equivalent to pCCD. These results clarify the role of pair-based ansätze and open avenues for hybrid approaches that combine the strengths of orbital- and geminal-based methods.

Published under an exclusive license by AIP Publishing. <https://doi.org/10.1063/5.0305612>

I. INTRODUCTION

Slater determinants, built from single-electron orbital wavefunctions, play a central role in quantum chemistry as the building blocks for most correlation treatments.¹ These include perturbation theory, configuration interaction (CI), multi-configurational self-consistent field (MCSCF), and coupled-cluster (CC) theory.^{1,2} Their widespread use is largely due to the efficiency of second quantization,^{3,4} which, along with practical tools such as Wick's theorem,^{5,6} facilitates theoretical developments and efficient computational implementations in electronic structure methods.^{1,7–11}

Despite their theoretical appeal, these approaches, while systematically improvable, often struggle to fully capture electron correlation in practice. Low-order methods such as MP2, CISD, and CCSD describe weak (dynamic) correlation well but fail to account for strong (static) correlation effects. Accurately treating strong correlation requires more advanced methods, such as complete active space self-consistent field (CASSCF),^{12–14} density matrix renormalization group (DMRG),^{15–20} higher-order CC methods (e.g., CCSDTQ),^{21,22} or selected CI approaches.^{23–28} However, the computational cost of these methods limits their application to relatively small systems.

An alternative perspective comes from geminal-based theories,^{29–32} which explicitly model electron pairing and offer a conceptually appealing way to describe strong correlation. Because of their direct connection to chemical bonding and Lewis structures,³³ geminal-based methods naturally capture strong correlation in bond-breaking and multi-reference problems.^{34–40} However, their implementation is challenging due to the complexity of handling geminal wavefunctions, and they often neglect weak correlation effects. As a result, electronic structure theory remains largely dominated by orbital- and density-based approaches.

Bridging the gap between orbital and geminal methods remains a key challenge in quantum chemistry. A deeper understanding of their connections may help develop hybrid approaches that combine the advantages of both; that is, retaining the systematic improvability of orbital-based methods while incorporating the robust treatment of strong correlation inherent in geminal theories.^{41–46}

The current push for pair theories stems from Ref. 47, which demonstrated that strongly correlated systems could be described efficiently in terms of CI expansions in which the Slater determinants were classified according to their number of unpaired electrons, their *seniority*, rather than their level of excitation from a given

reference. Seniority-zero CI, or doubly-occupied CI (DOCI), that is, a CI of Slater determinants with no unpaired electrons (or closed-shell determinants),^{31,48,49} was found to describe bond-breaking processes qualitatively with systematic improvement possible by adding seniorities two and four.^{50–54} Unfortunately, even seniority-zero CI has exponential cost, though a computationally inexpensive method was quickly developed with almost no loss in numerical accuracy. This was published as the antisymmetric product of 1-reference orbital geminals (AP1roG),³⁷ and was immediately understood to be equivalent to pair coupled-cluster doubles (pCCD).^{55,56} Seniority-zero methods, and hence pCCD, are not invariant to orbital rotations and thus require orbital optimization.^{56–62} As a result, the reference is *not* the Hartree–Fock (HF) Slater determinant. The optimal orbitals are generally localized on at most two atomic centers, resembling those from generalized valence bond (GVB) theory.⁶³ As defined by Dunning and co-workers,⁴⁶ GVB is a linear combination (i.e., a CI expansion) of all possible singlet-coupled configuration state functions (CSFs) in a given set of orbitals. This definition necessarily includes contributions from all possible seniorities. Usually, only a small number of CSFs are relevant, which leads to the practical approximation of *strongly orthogonal perfect pairs*. In this case, GVB simplifies to a *product* of singlet-coupled electron pairs: each coupling contains two spatial orbitals, and each spatial orbital appears in only one such coupling. In terms of atomic orbitals, this state is a product of Heitler–London-type states, while its natural orbitals are localized into sets of bonding and anti-bonding orbitals. Henceforth, we will only consider GVB with strongly orthogonal perfect pairs and refer to it as perfect-pairing (PP). PP is understood to describe strong correlation in bond-breaking processes.^{29,46,64–79} It has long been recognized that PP can be written as a CC wavefunction.^{41,80–85} More recently, PP-based ansätze have proven useful for maximizing the accuracy of shallow quantum circuits in the context of quantum computing.^{86–90}

In a previous paper,⁹¹ it was demonstrated that DOCI can be reduced to single-reference Epstein–Nesbet perturbation theory (ENPT),^{92,93} built from eigenvectors of the reduced Bardeen–Cooper–Schrieffer (BCS) Hamiltonian,^{94–96} the so-called Richardson–Gaudin (RG) states.^{97–100} In this paper, we first show that the reduced BCS Hamiltonian can be simplified to a form describing bonding/anti-bonding pairs of orbitals. PP emerges as an eigenvector of the simplified model, while the other eigenvectors provide a basis for PP's orthogonal complement. Weak correlation, in the PP picture, can then be accounted for systematically in a single-reference approach. In particular, it will be demonstrated that the corresponding second-order ENPT (EN2) PP-corrected energy is nearly equivalent to its pCCD counterpart.

II. THEORY

A. Perfect-pairing

First, we will fix our notation. We consider closed-shell systems composed of N electrons. Further, we assume there is no core, so that for a system with K spatial orbitals, the N electrons are distributed in N active spatial orbitals composed of bonding and antibonding pairs (see below), while the remaining $K - N$ spatial orbitals are labeled as virtuals. The indices $1 \leq p, q, r, s, \dots \leq N$ indicate active spatial orbitals, while the sets of indices $1 \leq i, j, k, l, \dots \leq N/2$ and $N/2 + 1 \leq a, b, c, d, \dots \leq N$ denote occupied and unoccupied active spatial

orbitals, respectively. The Greek letters $1 \leq \alpha, \beta, \gamma, \delta, \dots \leq N/2$ are reserved for orbital pairs, and $\sigma, \tau = \uparrow$ or \downarrow are spin labels. The letters μ, ν, λ will only refer to the bonding/antibonding labels, taking values 0 or 1.

Computations involving Slater determinants—many-electron wave functions written as antisymmetrized sums of products of one-electron orbitals—can be conveniently reduced to operations with creation (annihilation) operators \hat{a}_{pq}^\dagger (\hat{a}_{pq}), which add (remove) an electron in spatial orbital p with spin σ . These one-body operators fulfill the well-known anticommutation rules: $\{\hat{a}_{pq}^\dagger, \hat{a}_{qr}^\dagger\} = 0$, $\{\hat{a}_{pq}, \hat{a}_{qr}\} = 0$, and $\{\hat{a}_{pq}^\dagger, \hat{a}_{qr}\} = \delta_{pq}\delta_{\sigma\tau}$, where $\{\cdot, \cdot\}$ is the anticommutator.

Computations with pair (i.e., two-electron) wave functions, also known as geminals, are more involved but can be reduced to operations with three operators:

$$\hat{P}_p^+ = \hat{a}_{p\uparrow}^\dagger \hat{a}_{p\downarrow}^\dagger, \quad \hat{P}_p^- = \hat{a}_{p\downarrow} \hat{a}_{p\uparrow}, \quad \hat{n}_p = \hat{a}_{p\uparrow}^\dagger \hat{a}_{p\uparrow} + \hat{a}_{p\downarrow}^\dagger \hat{a}_{p\downarrow}, \quad (1)$$

where \hat{P}_p^+ (\hat{P}_p^-) creates (removes) a pair of opposite-spin electrons in the spatial orbital p , while \hat{n}_p counts the number of electrons in the spatial orbital p . These three operators have the structure of the Lie algebra su (2):

$$[\hat{P}_p^+, \hat{P}_q^-] = \delta_{pq}(\hat{n}_p - 1), \quad [\hat{n}_p, \hat{P}_q^\pm] = \pm 2\delta_{pq}\hat{P}_p^\pm. \quad (2)$$

The reduced BCS Hamiltonian,

$$\hat{H}_{\text{BCS}} = \frac{1}{2} \sum_p \xi_p \hat{n}_p + \frac{1}{2} \sum_{pq} \hat{P}_p^+ \hat{P}_q^-, \quad (3)$$

is an exactly solvable model describing pairs of electrons distributed among spatial orbitals with energies $\{\xi_p\}$ in a constant-strength interaction. Its eigenvectors, the RG states, are simply constructed from nonlinear equations. In previous papers,^{39,91,101–104} molecular systems were treated with RG states by variationally minimizing the energy of the Coulomb Hamiltonian:

$$\hat{H}_{\text{C}} = \sum_{pq} h_{pq} \sum_\sigma \hat{a}_{pq}^\dagger \hat{a}_{q\sigma} + \frac{1}{2} \sum_{pqrs} V_{pqrs} \sum_{\sigma\tau} \hat{a}_{pq}^\dagger \hat{a}_{qr}^\dagger \hat{a}_{st} \hat{a}_{q\sigma}, \quad (4)$$

where h_{pq} are elements of the one-electron Hamiltonian, and V_{pqrs} are direct two-electron integrals in Mulliken's, or chemists', notation, with respect to the parameters $\{\xi_p\}$. In other words, an optimal model Hamiltonian was identified that produced a state minimizing the energy of the real molecular system. The optimal $\{\xi_p\}$ found grouped the N spatial orbitals into $N/2$ well-separated subsystems, each consisting of near-degenerate bonding and antibonding orbitals that we will call valence-bond subsystems (VBS). This is illustrated in Fig. 1.

The reduced BCS Hamiltonian and its eigenvectors simplify dramatically when the VBS are treated as disjoint, leading to a collection of two-level systems that do not interact with one another. In other words, an *independent-pair approximation*. Each of the $\alpha = 1, \dots, N/2$ independent VBS contains a bonding spatial orbital α_0 and an antibonding spatial orbital α_1 (see Fig. 1). The number of pairs in each VBS is now a symmetry, and thus $\xi_{\alpha_0}(\hat{n}_{\alpha_0} + \hat{n}_{\alpha_1})$ is a

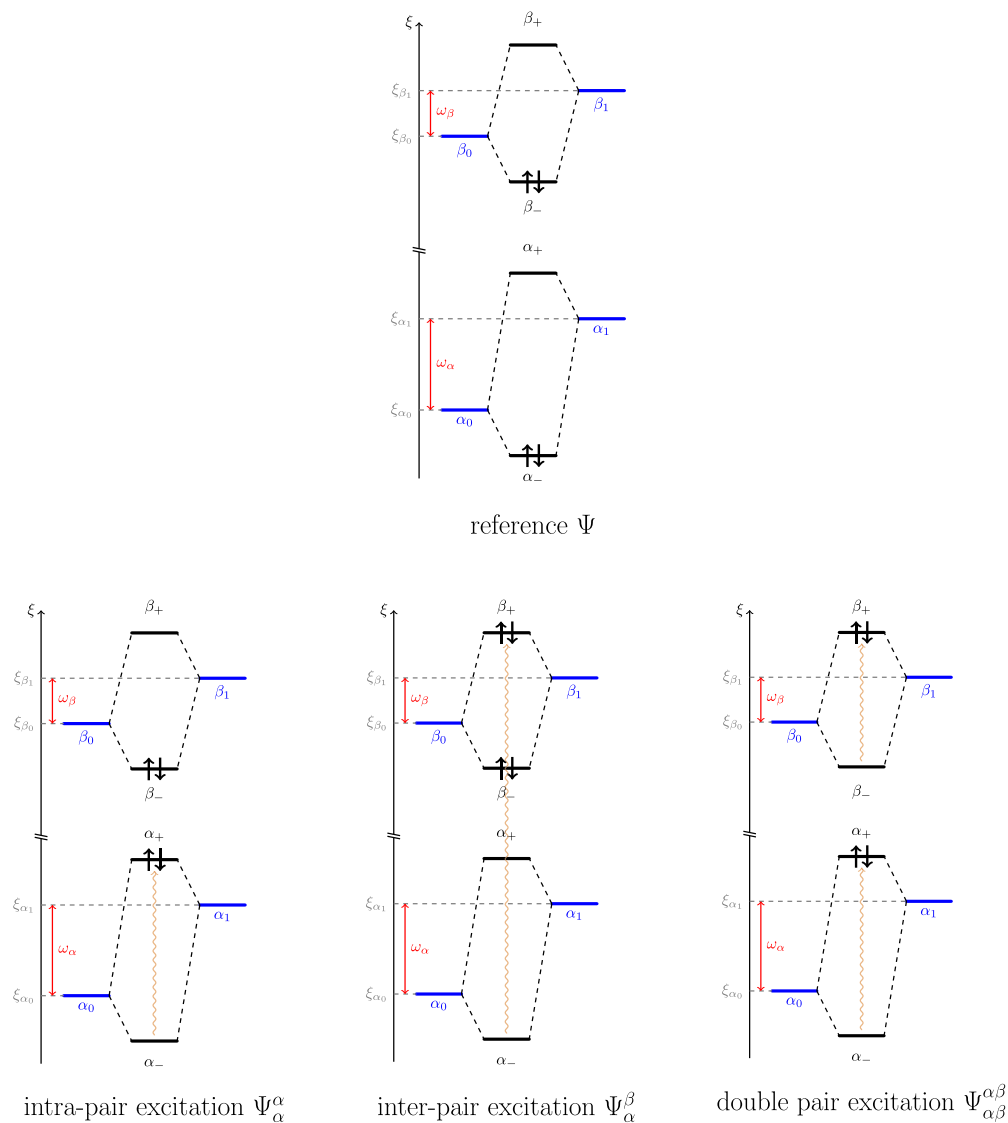


FIG. 1. Schematic representation of the orbital diagram in PP: reference PP wave function (top) and the three types of excited configurations (bottom). Here, we have represented two VBS, $\{\alpha_0, \alpha_1\}$ and $\{\beta_0, \beta_1\}$, characterized by VBS gaps $\omega_\alpha = \xi_{\alpha_1} - \xi_{\alpha_0}$ and $\omega_\beta = \xi_{\beta_1} - \xi_{\beta_0}$, respectively.

constant that can be removed, in addition to the diagonal terms of the interaction. The effective Hamiltonian is thus,

$$\hat{H}_{\text{PP}} = \frac{1}{2} \sum_{\alpha} \omega_{\alpha} \hat{n}_{\alpha_1} + \frac{1}{2} \sum_{\alpha} (\hat{P}_{\alpha_0}^+ \hat{P}_{\alpha_1}^- + \hat{P}_{\alpha_1}^+ \hat{P}_{\alpha_0}^-). \quad (5)$$

Pairs move between the bonding and antibonding orbitals with a constant strength, accounting for Coulomb repulsion, while electrons in the antibonding orbital increase the energy by the VBS gap $\omega_{\alpha} = \xi_{\alpha_1} - \xi_{\alpha_0}$. As Eq. (5) is a sum of disjoint contributions for each VBS, its eigenvectors factor into products of the eigenvectors of each VBS. In the seniority-zero sector, that is, in terms of only \hat{P}_p^+ , \hat{P}_p^- , and \hat{n}_p , each VBS has four eigenvectors: both orbitals can be empty $|0\rangle$, both orbitals can be doubly occupied $|\alpha_0 \alpha_1\rangle = \hat{P}_{\alpha_0}^+ \hat{P}_{\alpha_1}^+ |0\rangle$, or one

pair can be distributed among the two orbitals, and $|\alpha_0\rangle = \hat{P}_{\alpha_0}^+ |0\rangle$ and $|\alpha_1\rangle = \hat{P}_{\alpha_1}^+ |0\rangle$, in two ways,

$$|\alpha_{\pm}\rangle = |\alpha_0\rangle + \left(\omega_{\alpha} \pm \sqrt{\omega_{\alpha}^2 + 1} \right) |\alpha_1\rangle, \quad (6)$$

based on the value of ω_{α} , with norm

$$\mathcal{N}_{\alpha_{\pm}} = \langle \alpha_{\pm} | \alpha_{\pm} \rangle = 2\sqrt{\omega_{\alpha}^2 + 1} \left(\sqrt{\omega_{\alpha}^2 + 1} \pm \omega_{\alpha} \right). \quad (7)$$

The weights of $|\alpha_0\rangle$ and $|\alpha_1\rangle$ in Eq. (6) are chosen so that in the degenerate limit (i.e., $\omega_{\alpha} \rightarrow 0$), these two states become strict symmetric/antisymmetric linear combinations $(|\alpha_0\rangle \pm |\alpha_1\rangle)/\sqrt{2}$. For $|\alpha_-\rangle$, the bonding orbital is more strongly occupied, and the product

$$|\Psi\rangle = \prod_{\alpha} |\alpha_{-}\rangle, \quad (8)$$

is the state traditionally called PP¹⁰⁵ (see Fig. 1). It is an eigenvector of Eq. (5), almost always the ground state. [If $\omega_{\alpha} \ll \omega_{\beta}$, the configuration $|\alpha_0\alpha_1\rangle$ is energetically more favorable than $|\alpha_{-}\beta_{-}\rangle$. For molecular systems, this does not happen, and $|\Psi\rangle$ is the ground state of Eq. (5).]

With $\mu \in \{0, 1\}$, the one-electron reduced density matrix (1-RDM) elements are explicit functions of the VBS gaps:

$$n_{\alpha_{\mu}} = \frac{1}{2} \frac{\langle \Psi | \hat{n}_{\alpha_{\mu}} | \Psi \rangle}{\langle \Psi | \Psi \rangle} = \frac{1}{2} \left[1 + \frac{(-1)^{\mu} \omega_{\alpha}}{\sqrt{\omega_{\alpha}^2 + 1}} \right], \quad (9)$$

(with $0 \leq n_{\alpha_{\mu}} \leq 1$ and $n_{\alpha_0} + n_{\alpha_1} = 1$) while there are two types of two-electron reduced density matrix (2-RDM) elements. The pair-transfer elements are non-zero only within a VBS:

$$P_{\alpha_0\alpha_1} = \frac{\langle \Psi | \hat{P}_{\alpha_0}^{+} \hat{P}_{\alpha_1}^{-} | \Psi \rangle}{\langle \Psi | \Psi \rangle} = -\sqrt{n_{\alpha_0} n_{\alpha_1}} = -\frac{1}{2} \frac{1}{\sqrt{\omega_{\alpha}^2 + 1}}, \quad (10)$$

and $P_{\alpha_{\mu}\alpha_{\mu}} = +n_{\alpha_{\mu}}$. The density-density elements are non-zero only between distinct VBS (i.e., $\alpha \neq \beta$):

$$D_{\alpha_{\mu}\beta_{\nu}} = \frac{1}{4} \frac{\langle \Psi | \hat{n}_{\alpha_{\mu}} \hat{n}_{\beta_{\nu}} | \Psi \rangle}{\langle \Psi | \Psi \rangle} = n_{\alpha_{\mu}} n_{\beta_{\nu}}. \quad (11)$$

As $P_{\alpha_{\mu}\alpha_{\nu}}$ is non-zero only within a VBS and $D_{\alpha_{\mu}\beta_{\nu}}$ is reducible, there is no correlation between electron pairs for PP: the 2-RDM elements are explicit functions of the 1-RDM elements.^{106,107} As the 1-RDM elements (9) are themselves explicit functions of $\{\omega_{\alpha}\}$, the PP energy of the Coulomb Hamiltonian (4),

$$\begin{aligned} E[\{\omega_{\alpha}\}] = & 2 \sum_{\alpha} \sum_{\mu} n_{\alpha_{\mu}} \left(h_{\alpha_{\mu}\alpha_{\mu}} + \frac{1}{2} L_{\alpha_{\mu}\alpha_{\mu}} \right) + 2 \sum_{\alpha} P_{\alpha_0\alpha_1} L_{\alpha_0\alpha_1} \\ & + 2 \sum_{\alpha<\beta} \sum_{\mu\nu} D_{\alpha_{\mu}\beta_{\nu}} G_{\alpha_{\mu}\beta_{\nu}}, \end{aligned} \quad (12)$$

can be minimized variationally with respect to the VBS gaps $\{\omega_{\alpha}\}$. Here, the two-electron integrals reduce to direct (J), exchange (K), and pair-transfer (L) types:

$$J_{\alpha_{\mu}\beta_{\nu}} = V_{\alpha_{\mu}\alpha_{\mu}\beta_{\nu}\beta_{\nu}}, \quad (13a)$$

$$K_{\alpha_{\mu}\beta_{\nu}} = V_{\alpha_{\mu}\beta_{\nu}\beta_{\nu}\alpha_{\mu}}, \quad (13b)$$

$$L_{\alpha_{\mu}\beta_{\nu}} = V_{\alpha_{\mu}\beta_{\nu}\alpha_{\mu}\beta_{\nu}}. \quad (13c)$$

For real orbitals, the exchange and pair-transfer integrals are identical. The three summations in Eq. (12) represent the one-body terms, the pair-transfer elements, and the density-density elements, respectively. The direct and exchange integrals always occur together, so we adopt the shorthand:

$$G_{\alpha_{\mu}\beta_{\nu}} = 2J_{\alpha_{\mu}\beta_{\nu}} - K_{\alpha_{\mu}\beta_{\nu}}. \quad (14)$$

We choose to write the diagonal two-electron integral $L_{\alpha_{\mu}\alpha_{\mu}} = V_{\alpha_{\mu}\alpha_{\mu}\alpha_{\mu}\alpha_{\mu}}$.

To perform such a minimization, we rely on the Newton-Raphson algorithm, which requires the first (gradient),

$$\left(\omega_{\alpha}^2 + 1 \right)^{\frac{3}{2}} \frac{\partial E}{\partial \omega_{\alpha}} = \omega_{\alpha} L_{\alpha_0\alpha_1} + \sum_{\mu} (-1)^{\mu} \left(h_{\alpha_{\mu}\alpha_{\mu}} + \frac{1}{2} L_{\alpha_{\mu}\alpha_{\mu}} \right. \\ \left. + \sum_{\beta(\neq\alpha)} \sum_{\nu} G_{\alpha_{\mu}\beta_{\nu}} n_{\beta_{\nu}} \right), \quad (15)$$

and second (Hessian) derivatives of the energy with respect to the VBS gaps:

$$\left(\omega_{\alpha}^2 + 1 \right)^{\frac{3}{2}} \left(\omega_{\beta}^2 + 1 \right)^{\frac{3}{2}} \frac{\partial^2 E}{\partial \omega_{\alpha} \partial \omega_{\beta}} = \frac{1}{2} \sum_{\mu\nu} (-1)^{\mu+\nu} G_{\alpha_{\mu}\beta_{\nu}}, \quad (16a)$$

$$\left(\omega_{\alpha}^2 + 1 \right)^{\frac{3}{2}} \frac{\partial E^2}{\partial \omega_{\alpha}^2} = -3\omega_{\alpha} \left(\omega_{\alpha}^2 + 1 \right)^{\frac{1}{2}} \frac{\partial E}{\partial \omega_{\alpha}} + L_{\alpha_0\alpha_1}. \quad (16b)$$

Thus, for a given set of orbitals, the electronic gradient [see Eq. (15)] and the electronic Hessian [see Eq. (16)] are constructed with $\mathcal{O}(N^2)$ operations, which are cheaper than the linear algebra operations required for the Newton-Raphson steps.

Requiring the gradient to vanish implies

$$\sum_{\mu} (-1)^{\mu} \left(h_{\alpha_{\mu}\alpha_{\mu}} + \frac{1}{2} L_{\alpha_{\mu}\alpha_{\mu}} + \sum_{\beta(\neq\alpha)} \sum_{\nu} G_{\alpha_{\mu}\beta_{\nu}} n_{\beta_{\nu}} \right) = -\omega_{\alpha} L_{\alpha_0\alpha_1}, \quad (17)$$

a property that will have consequences in perturbation theory (see below). Equation (17) gives a physical meaning to the VBS gaps: the left-hand side of Eq. (17) is a difference of orbital energies defined as

$$\varepsilon_{\alpha_{\mu}} = h_{\alpha_{\mu}\alpha_{\mu}} + \frac{1}{2} L_{\alpha_{\mu}\alpha_{\mu}} + \sum_{\beta(\neq\alpha)} \sum_{\nu} G_{\alpha_{\mu}\beta_{\nu}} n_{\beta_{\nu}}, \quad (18)$$

while $L_{\alpha_0\alpha_1}$ in the right-hand side of Eq. (17) is the energy pushing a pair from the bonding orbital to the antibonding orbital. Here, the orbital energies are distinct from those obtained from HF as they include occupation numbers between 0 and 1. Orbital energies have likewise been defined in various ways for pCCD.¹⁰⁸

The stationary VBS gaps are thus ratios of the differences in orbital energies to the Coulomb repulsion,

$$\omega_{\alpha} = \frac{\varepsilon_{\alpha_1} - \varepsilon_{\alpha_0}}{L_{\alpha_0\alpha_1}}, \quad (19)$$

just as they are in the model Hamiltonian (5). The stationary PP energy can then be recast:

$$\begin{aligned} E = & \sum_{\alpha} \left[\varepsilon_{\alpha_0} + \varepsilon_{\alpha_1} + (\varepsilon_{\alpha_0} - \varepsilon_{\alpha_1}) \sqrt{1 + \left(\frac{L_{\alpha_0\alpha_1}}{\varepsilon_{\alpha_1} - \varepsilon_{\alpha_0}} \right)^2} \right] \\ & - 2 \sum_{\alpha<\beta} \sum_{\mu\nu} n_{\alpha_{\mu}} n_{\beta_{\nu}} G_{\alpha_{\mu}\beta_{\nu}}, \end{aligned} \quad (20)$$

similar to an expression obtained by Kutzelogg¹⁰⁹ for a two-level problem in particular. Equation (20) reduces to the stationary HF energy when the VBS gaps $\{\omega_{\alpha}\}$ become large.¹¹⁰

Unfortunately, orbital optimization is necessary for pair wavefunctions.^{56–59,111} One must also compute the first and second derivatives of the energy with respect to the orbital rotation parameters $\{\kappa_{pq}\}$. A unitary transformation of the orbitals,

$$\hat{U} = \exp \left[\sum_{p < q} \kappa_{pq} \sum_{\sigma} (\hat{a}_{p\sigma}^{\dagger} \hat{a}_{q\sigma} - \hat{a}_{q\sigma}^{\dagger} \hat{a}_{p\sigma}) \right], \quad (21)$$

may be constructed as a step away from the identity $\kappa = 0$. In this case, the gradient and Hessian simplify to expectation values of commutators.¹ The orbital gradient,

$$\frac{\partial E}{\partial \kappa_{pq}} = 4h_{pq}(n_p - n_q) + 4 \sum_r (2V_{rrpq} - V_{rqpr})(D_{rp} - D_{rq}) \\ + 4 \sum_r V_{rprq}(P_{rp} - P_{rq}), \quad (22)$$

and Hessian,

$$\frac{\partial^2 E}{\partial \kappa_{pq} \partial \kappa_{rs}} = 4(P_{pr} - P_{ps} + P_{qs} - P_{qr})(V_{qrps} + V_{qspr}) \\ + 4(D_{pr} - D_{ps} + D_{qs} - D_{qr})(4V_{qprs} - V_{qrps} - V_{qsrp}) \\ + \delta_{pr}[(4n_p - 2n_q - 2n_s)h_{qs} + W_{pqrs}] \\ + \delta_{qs}[(4n_q - 2n_p - 2n_r)h_{pr} + W_{qpr}] \\ - \delta_{ps}[(4n_p - 2n_q - 2n_r)h_{qr} + W_{pqr}] \\ - \delta_{qr}[(4n_q - 2n_p - 2n_s)h_{ps} + W_{qps}], \quad (23)$$

are both computed from the RDM elements. The Hessian is efficiently computed from the intermediates,

$$W_{pqr} = 2 \sum_s (2P_{ps} - P_{qs} - P_{rs})V_{qssr} \\ + 2 \sum_s (2D_{ps} - D_{qs} - D_{rs})(2V_{qrss} - V_{qssr}), \quad (24)$$

which requires $\mathcal{O}(N^3)$ storage. The mixed elements of the Hessian occur in three types. For the first, the VBS gap ω_y does not correspond to one of the orbitals being rotated:

$$(\omega_y^2 + 1)^{\frac{3}{2}} \frac{\partial^2 E}{\partial \omega_y \partial \kappa_{\alpha_\mu \beta_\nu}} = 2 \sum_{\lambda} (-1)^{\lambda} (2V_{\gamma\gamma\lambda\alpha_\mu\beta_\nu} - V_{\gamma\lambda\beta_\nu\alpha_\mu\gamma_\lambda}) \\ \times (n_{\alpha_\mu} - n_{\beta_\nu}), \quad (25)$$

while the remaining two types are

$$(\omega_\alpha^2 + 1)^{\frac{3}{2}} \frac{\partial^2 E}{\partial \omega_\alpha \partial \kappa_{\alpha_\mu \beta_\nu}} = 2\omega_\alpha V_{\alpha_1 \dots \alpha_\mu \alpha_{1-\mu} \beta_\nu} \\ + 2(-1)^\mu [Q_{\alpha_\mu \beta_\nu} + V_{\alpha_\mu \alpha_\mu \alpha_\mu \beta_\nu}] \\ - 2 \sum_{\lambda} (2V_{\alpha_\lambda \alpha_\lambda \alpha_\mu \beta_\nu} - V_{\alpha_\lambda \beta_\nu \alpha_\mu \alpha_\lambda}) \\ \times [(-1)^\mu n_{\alpha_\lambda} + (-1)^\lambda n_{\beta_\nu}], \quad (26a)$$

$$(\omega_\beta^2 + 1)^{\frac{3}{2}} \frac{\partial^2 E}{\partial \omega_\beta \partial \kappa_{\alpha_\mu \beta_\nu}} = -2\omega_\beta V_{\beta_1 \dots \beta_\nu \alpha_\mu \beta_{1-\nu} \beta_\nu} \\ - 2(-1)^\nu [Q_{\alpha_\mu \beta_\nu} + V_{\beta_\nu \beta_\nu \beta_\nu \alpha_\mu}] \\ + 2 \sum_{\lambda} (2V_{\beta_\lambda \beta_\lambda \alpha_\mu \beta_\nu} - V_{\beta_\lambda \beta_\nu \alpha_\mu \beta_\lambda}) \\ \times [(-1)^\lambda n_{\alpha_\mu} + (-1)^\nu n_{\beta_\lambda}]. \quad (26b)$$

The full Hessian can be constructed with $\mathcal{O}(N^4)$ operations, so the scaling bottleneck for orbital-optimized PP (OO-PP) will, in

principle, be the $\mathcal{O}(N^5)$ transformation of the two-electron integrals.¹¹² The orbital gradient (22) and orbital Hessian (23) are valid for any seniority-zero wavefunction, provided the density matrices n , D , and P . While in this contribution we consider PP only in the valence, core ($n_i = 1$) and virtual ($n_a = 0$) orbitals may be added without too much difficulty. Density-density 2-RDM elements involving core and virtual orbitals factor into products of occupation numbers [see Eq. (11)], while pair-transfer elements vanish. The orbital gradient (22) will therefore vanish for core–core and virtual–virtual rotations, making PP invariant to such transformations.

Rather than building the complete Hessian, stationary equations are available for the orbital coefficients for the antisymmetrized product of strongly-orthogonal geminals (APSG), a more general structure than PP.^{113,114} This is the traditional approach for PP^{115,116} that also employs two coefficients, and thus a constraint, for each pair rather than the VBS gaps $\{\omega_\alpha\}$. In the end, the scaling is the same, the VBS gaps remove redundancies and have clear physical meanings, and the complete Hessian is computable. We feel the current approach is more transparent.

Variational OO-PP is a *mean-field of non-interacting pairs*, and the model Hamiltonian (5) provides a basis for the Hilbert space to account for the outstanding weak correlation (relative to PP). In the seniority-zero sector, $|\Psi\rangle$ couples to three types of excitations through \hat{H}_C , as shown in Fig. 1. In each VBS α , the process $|\alpha_-\rangle \rightarrow |\alpha_+\rangle$ is called an *intra-pair excitation* and denoted $|\Psi_\alpha^\alpha\rangle$. An *inter-pair excitation* $|\Psi_\alpha^\beta\rangle$ from α to β refers to $|\alpha_-\rangle \rightarrow |\beta_0 \beta_1\rangle$. Finally, a *double-pair excitation* $|\Psi_{\alpha\beta}^{\alpha\beta}\rangle$ refers to $|\alpha_-\rangle \rightarrow |\alpha_+ \beta_+\rangle$. Additional couplings were possible for RG states, while they are totally forbidden for PP. A CI treatment of PP with its singles and doubles (CISD) is possible, though in Ref. 91 it was found for RG states that EN2 was much more attractive: building the RG-based CISD matrix cost $\mathcal{O}(N^8)$ operations, while EN2 cost only $\mathcal{O}(N^6)$. For the dissociation of linear H₈, the maximum disagreement between the two methods was about $2 \times 10^{-5} E_h$ for very short interatomic distances, and this disagreement went to zero quickly as the distance increased. In any case, the CISD treatment of PP was performed to verify that our expressions were correct.

Here, an EN reference Hamiltonian can be written as

$$\hat{H}_0 = |\Psi\rangle\langle\Psi|\hat{H}_C|\Psi\rangle\langle\Psi| + \sum_{\alpha\beta} |\Psi_\alpha^\beta\rangle\langle\Psi_\alpha^\beta|\hat{H}_C|\Psi_\alpha^\beta\rangle\langle\Psi_\alpha^\beta| \\ + \sum_{\alpha<\beta} |\Psi_{\alpha\beta}^{\alpha\beta}\rangle\langle\Psi_{\alpha\beta}^{\alpha\beta}|\hat{H}_C|\Psi_{\alpha\beta}^{\alpha\beta}\rangle\langle\Psi_{\alpha\beta}^{\alpha\beta}|, \quad (27)$$

with internal space $|\Psi\rangle$ and external space built from intra-pair, inter-pair, and double-pair excitations (see Fig. 1). The first-order correction to the energy is zero, while the second-order correction is

$$E^{(2)} = \sum_{\alpha\beta} \frac{|\langle\Psi_\alpha^\beta|\hat{H}_C|\Psi\rangle|^2}{E^{(0)} - E_\alpha^\beta} + \sum_{\alpha<\beta} \frac{|\langle\Psi_{\alpha\beta}^{\alpha\beta}|\hat{H}_C|\Psi\rangle|^2}{E^{(0)} - E_{\alpha\beta}^{\alpha\beta}}, \quad (28)$$

where $E^{(0)} = \langle\Psi|\hat{H}_C|\Psi\rangle$, $E_\alpha^\beta = \langle\Psi_\alpha^\beta|\hat{H}_C|\Psi_\alpha^\beta\rangle$, and $E_{\alpha\beta}^{\alpha\beta} = \langle\Psi_{\alpha\beta}^{\alpha\beta}|\hat{H}_C|\Psi_{\alpha\beta}^{\alpha\beta}\rangle$. This correction is simplified in the Appendix, leading to an evaluation of Eq. (28) with $\mathcal{O}(N^2)$ operations—essentially free once the OO-PP mean-field is constructed. Intra-pair excitations do not contribute at all: as shown in the Appendix, the

transition $\langle \Psi_\alpha^\alpha | \hat{H}_C | \Psi \rangle$ is equivalent to the gradient condition (17) and therefore vanishes. This is analogous to the Brillouin theorem within HF theory.¹¹⁷ This EN2 treatment includes only the seniority-zero sector as the goal is to compare with pCCD. An EN2 correction including PP excited states of non-zero seniorities will be computed in a future contribution, in the same manner as for RG states.^{118,119}

The natural orbital functions of Piris are also directly related to PP. At half-filling, the PNOF5¹⁰⁶ functional is equivalent to PP. Otherwise, it is equivalent to APSG.¹⁰⁷ For strong correlation, the best-performing functional is PNOF7,^{120,121} which can be seen as an update to PNOF5:

$$E_{\text{PNOF7}} = E_{\text{PNOF5}} + \Delta E_{\text{PNOF7}}. \quad (29)$$

Usually, PNOF7 is treated as a mean-field, solved with Lagrange multipliers in an SCF-like procedure, but PNOF7 is not N -representable. PNOF5, being equivalent to PP, is N -representable and variational. Thus, PNOF7 could be computed as a perturbative update to the variational PNOF5. In the present language, this update becomes

$$\Delta E_{\text{PNOF7}} = -\frac{1}{4} \sum_{\alpha} \sum_{\beta(\neq\alpha)} \frac{1}{(\omega_\alpha^2 + 1)^{\frac{1}{2}} (\omega_\beta^2 + 1)^{\frac{1}{2}}} \sum_{\mu} \sum_{\nu} L_{\alpha\mu} \beta_{\nu}. \quad (30)$$

B. Pair coupled-cluster doubles

We now move on to describe the connection with pCCD. The pCCD energy is very similar to the EN2-corrected PP energy. This can be evidenced by examining the pCCD wavefunction ansatz, which, in its most conventional form, reads

$$|\Phi_{\text{pCCD}}\rangle = e^{\hat{T}} |\Phi\rangle, \quad (31)$$

where

$$\hat{T} = \sum_{ia} t_i^\alpha \hat{P}_a^+ \hat{P}_i^- \quad (32)$$

is the cluster operator (which is restricted to paired double excitations at the pCCD level), and

$$|\Phi\rangle = \prod_{\alpha} |\alpha_0\rangle \quad (33)$$

is the closed-shell ground-state Slater determinant in which all the bonding orbitals are doubly occupied. As the orbitals are optimized from the bifunctional expression of the pCCD energy, the Slater determinant of bonding orbitals is *not* the HF Slater determinant. The pCCD state can be recast as

$$\begin{aligned} |\Phi_{\text{pCCD}}\rangle &= \exp \left(\sum_{\alpha\beta} t_\alpha^\beta \hat{P}_{\beta_1}^+ \hat{P}_{\alpha_0}^- \right) |\Phi\rangle \\ &= \exp \left(\sum_{\beta(\neq\alpha)} t_\alpha^\beta \hat{P}_{\beta_1}^+ \hat{P}_{\alpha_0}^- \right) \exp \left(\sum_{\alpha} t_\alpha^\alpha \hat{P}_{\alpha_1}^+ \hat{P}_{\alpha_0}^- \right) |\Phi\rangle, \end{aligned} \quad (34)$$

in terms of amplitudes t_α^β to be determined from a set of nonlinear equations obtained by projecting the Schrödinger equation onto the excited Slater determinants $|\Phi_\alpha^\beta\rangle = \hat{P}_{\beta_1}^+ \hat{P}_{\alpha_0}^- |\Phi\rangle$ from the left, as follows:

$$\langle \Phi_\alpha^\beta | \hat{H} | \Phi \rangle = 0, \quad (35)$$

where $\hat{H} = e^{-\hat{T}} \hat{H}_C e^{\hat{T}}$ is the similarity-transformed Hamiltonian. Splitting the exponential into diagonal and off-diagonal pieces is possible and makes the individual contributions evident: the diagonal cluster amplitudes will turn $|\Phi\rangle$ into $|\Psi\rangle$, that is,

$$\begin{aligned} |\Psi\rangle &= \exp \left(\sum_{\alpha} t_\alpha^\alpha \hat{P}_{\alpha_1}^+ \hat{P}_{\alpha_0}^- \right) |\Phi\rangle = \prod_{\alpha} \exp \left(t_\alpha^\alpha \hat{P}_{\alpha_1}^+ \hat{P}_{\alpha_0}^- \right) |\Phi\rangle \\ &= \prod_{\alpha} (1 + t_\alpha^\alpha \hat{P}_{\alpha_1}^+ \hat{P}_{\alpha_0}^-) |\Phi\rangle, \end{aligned} \quad (36)$$

while the off-diagonal cluster amplitudes will add the inter-pair excitations. Double-pair excitations will be approximated as products of the cluster amplitudes.

First, the diagonal cluster amplitudes transform $|\Phi\rangle$ into $|\Psi\rangle$. From Eq. (35), the (quadratic) amplitude equations for the right amplitudes $\{t_i^\alpha\}$ are⁵⁶

$$\begin{aligned} 0 = L_{ai} + 2 &\left(f_{aa} - f_{ii} - \sum_j L_{ja} t_j^a - \sum_b L_{ib} t_i^b \right) t_i^a - 2(2J_{ia} - K_{ia} - L_{ia} t_i^a) t_i^a \\ &+ \sum_b L_{ba} t_i^b + \sum_j L_{ji} t_j^a + \sum_{jb} L_{jb} t_j^a t_i^b, \end{aligned} \quad (37)$$

where f_{pq} are the elements of the Fock operator. In the single-pair approximation, it reduces to the following simple form:

$$1 + 2\omega_\alpha t_\alpha^\alpha - (t_\alpha^\alpha)^2 = 0, \quad (38)$$

with

$$\begin{aligned} \omega_\alpha &= \frac{f_{\alpha_1\alpha_1} - f_{\alpha_0\alpha_0} - 2J_{\alpha_0\alpha_1} + K_{\alpha_0\alpha_1} + \frac{L_{\alpha_0\alpha_0} + L_{\alpha_1\alpha_1}}{2}}{L_{\alpha_0\alpha_1}} \\ &= \frac{h_{\alpha_1\alpha_1} + \frac{L_{\alpha_1\alpha_1}}{2} - h_{\alpha_0\alpha_0} - \frac{L_{\alpha_0\alpha_0}}{2}}{L_{\alpha_0\alpha_1}}, \end{aligned} \quad (39)$$

which matches the expression obtained from Eq. (17) in the single-pair approximation. The ground-state amplitude for the pair α is thus simply given by

$$t_\alpha^\alpha = \omega_\alpha - \sqrt{1 + \omega_\alpha^2} = -\sqrt{\frac{n_{\alpha_1}}{n_{\alpha_0}}}, \quad (40)$$

which corresponds to the state $|\alpha_-\rangle$. As Eq. (38) is quadratic, there is evidently a second root corresponding to the state $|\alpha_+\rangle$. The pCCD energy is defined via the following energy bi-functional:⁵⁶

$$E_{\text{pCCD}} = \langle \Phi | (1 + \hat{Z}) \hat{H} | \Phi \rangle, \quad (41)$$

where $\hat{Z} = \sum_{ia} z_a^\alpha \hat{P}_a^+ \hat{P}_a^-$ is a de-excitation operator. The (linear) amplitude equations for the left amplitudes $\{z_a^\alpha\}$ are⁵⁶

$$\begin{aligned} 0 = L_{ia} + 2 &\left(f_{aa} - f_{ii} - \sum_j L_{ja} t_j^a - \sum_b L_{ib} t_i^b \right) z_a^\alpha - 2(2J_{ia} - K_{ia} \\ &- 2L_{ia} t_i^a) z_a^\alpha + \sum_b L_{ab} z_b^\alpha + \sum_j L_{ij} z_j^\alpha + \sum_{jb} t_j^b (L_{ib} z_a^\alpha + L_{ja} z_b^\alpha) \\ &- 2L_{ia} \left(\sum_j z_j^\alpha t_j^a + \sum_b z_b^\alpha t_i^b \right). \end{aligned} \quad (42)$$

In the single-pair approximation, it reduces to the following simple form:

$$1 + 2(\omega_\alpha - t_\alpha^\alpha)z_\alpha^\alpha = 0. \quad (43)$$

The left ground-state amplitude for the pair α is thus,

$$z_\alpha^\alpha = -\frac{1}{2(\omega_\alpha - t_\alpha^\alpha)} = -\sqrt{n_{\alpha_0} n_{\alpha_1}}, \quad (44)$$

where t_α^α is given by Eq. (40). The left and right amplitudes are then employed to compute the 1- and 2-RDM and, eventually, the energy. For example, the non-zero elements of the 1-RDM (which is diagonal at the pCCD level) are

$$n_i = \left(1 - \sum_a t_i^a z_a^i\right), \quad (45a)$$

$$n_a = \sum_i t_i^a z_a^i. \quad (45b)$$

In the single-pair approximation, it is easily shown that one recovers the expressions of Eq. (9). Likewise, for the elements of the 2-RDM P (hence the energy), while the elements of D vanish in the single-pair approximation. This slightly generalizes Cullen's derivation⁴¹ and shows that, within the single-pair approximation, pCCD and PP are strictly equivalent. However, it does not demonstrate the equivalence of these two formalisms beyond the single-pair approximation.

III. NUMERICAL RESULTS

To illustrate the theoretical results discussed above, we consider chains of (equidistant) hydrogen atoms of increasing size at half-filling, which here corresponds to the minimal basis STO-6G. Of course, PP can include core and virtual orbitals, but that is not the present purpose. As OO-PP, OO-PP-EN2, and OO-pCCD are seniority-zero states, results are compared with OO-DOCI. In all

cases, we report *reduced energies*, that is, the energy divided by the number of electrons.

OO-PP results were computed using the Newton-Raphson algorithm by constructing the full Hessian. Symmetric and antisymmetric linear combinations of the 1s hydrogen orbitals on neighboring sites served as a sufficient initial guess for the orbitals, while the VBS gaps were initialized to values smaller than one. In general, for distances larger than $R_{\text{H-H}} = 2.5 a_0$, this approach converges in 3–4 iterations. At shorter distances, the Hessian develops negative eigenvalues, and we adopt a level-shift approach to ensure the Hessian remains positive definite. The time spent computing the EN2 correction is negligible in comparison. The pCCD calculations were performed using the same methodology as in Ref. 122 with the MOLGW program,¹²³ which incorporates the stand-alone NOFT module¹²⁴ based on the DoNOF program.¹²⁵

RHF and FCI results were obtained with PySCF,¹²⁶ while OO-DOCI results were computed with our own code. OO-DOCI convergence is difficult near the minimum: the optimization is decoupled, switching between exact diagonalization of the DOCI Hamiltonian matrix and Newton-Raphson optimization of the orbital coefficients. More robust and efficient optimization strategies have been proposed in the literature.^{127–129}

First, we consider the smallest non-trivial chain H_4 , and the results are presented in Fig. 2. It is difficult to visually discern the reduced energies of OO-PP, OO-PP-EN2, OO-pCCD, and OO-DOCI, so only the OO-DOCI curve is plotted in the left panel of Fig. 2. Indeed, one can see in the right panel of Fig. 2 that the respective errors, in terms of reduced energies, for the three approximate methods are below 1 mE_h per electron everywhere. As OO-PP is a variational approximation, it is always above OO-DOCI. OO-PP-EN2 is above OO-DOCI until $R_{\text{H-H}} = 3.1 a_0$, where it falls below OO-DOCI. OO-pCCD is always below OO-DOCI. At short distances, OO-pCCD performs best but is quickly overtaken by OO-PP-EN2 and even OO-PP. As it has an exponential parametrization, pCCD is extensive, as is PP due to Eq. (36). The OO-PP-EN2 correction goes to zero rapidly for distinct subsystems as the optimal orbitals are localized.⁶³ A detailed analysis of the extensivity of

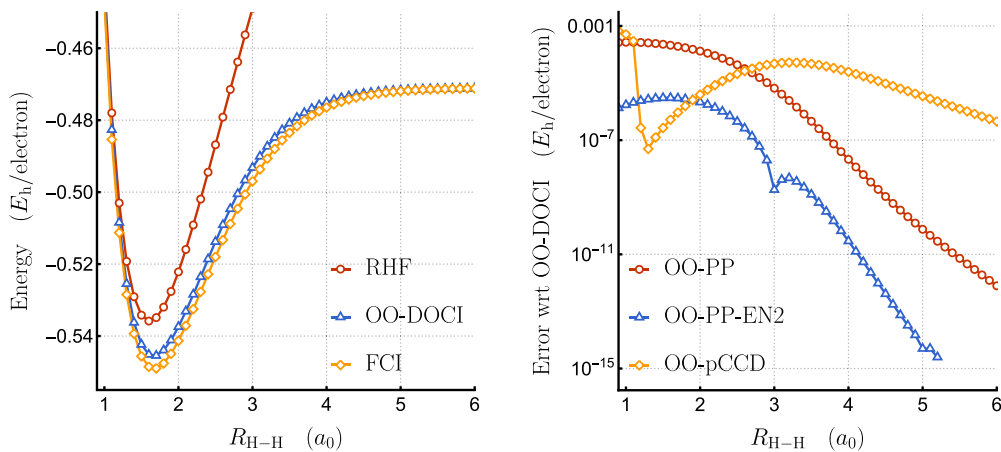


FIG. 2. Symmetric dissociation of H_4 chain in STO-6G. Orbitals were optimized separately for PP, pCCD, and DOCI. Left: reduced energies for RHF, OO-DOCI, and FCI. Right: absolute errors of OO-PP, OO-PP-EN2, and OO-pCCD with respect to OO-DOCI plotted logarithmically. OO-PP-EN2 is above OO-DOCI until $R_{\text{H-H}} = 3.1 a_0$, where it goes below and overcorrelates the rest of the way to dissociation. OO-pCCD always overcorrelates relative to OO-DOCI.

TABLE I. Reduced energies computed at $R_{\text{H-H}} = 1.6 a_0$, near the equilibrium point. Each column represents a set of orbitals, while each row is a method. All results computed in STO-6G.

Method	Orbital set		
	PP	pCCD	DOCI
PP	-0.544 92	-0.544 92	-0.544 92
PP-EN2	-0.545 13	-0.545 13	-0.545 13
pCCD	-0.545 13	-0.545 13	-0.545 13
DOCI	-0.545 13	-0.545 13	-0.545 13

TABLE II. Reduced energies computed at $R_{\text{H-H}} = 3.2 a_0$. Each column represents a set of orbitals, while each row is a method. All results computed in STO-6G.

Method	Orbital set		
	PP	pCCD	DOCI
PP	-0.487 28	-0.487 28	-0.487 28
PP-EN2	-0.487 28	-0.487 28	-0.487 28
pCCD	-0.487 33	-0.487 33	-0.487 33
DOCI	-0.487 28	-0.487 28	-0.487 28

the EN2 correction is presented in Ref. 91. Evidently, the energy differences among these methods are very small and are unlikely to be significant in practical applications.

To better demonstrate how small the energy differences between the methods are, reduced energies for PP, EN2, pCCD, and DOCI were computed in the OO-PP, OO-pCCD, and OO-DOCI orbitals. The reduced energies at $R_{\text{H-H}} = 1.6 a_0$, near equilibrium, are shown in Table I. This point is chosen as it represents where weak correlation is dominant. Here, EN2 and pCCD are identical to DOCI. PP is slightly above, as it misses the weak correlation.

Reduced energies for each method in each set of orbitals at $R_{\text{H-H}} = 3.2 a_0$ are reported in Table II. At this point, the VBS gaps are both less than 1, indicating that the Coulomb repulsion is larger

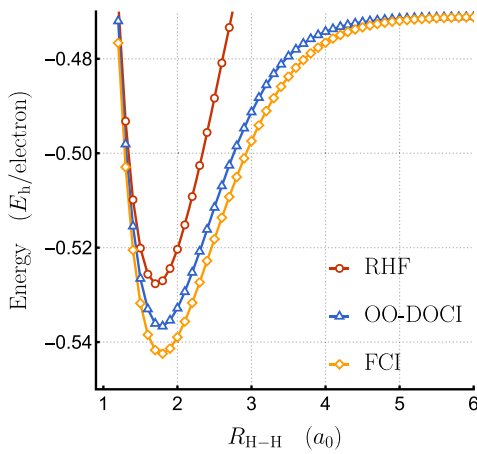


FIG. 3. Symmetric dissociation of H_{10} chain in STO-6G. Orbitals were optimized separately for PP, pCCD, and DOCI. Left: reduced energies for RHF, OO-DOCI, and FCI. Right: absolute errors of OO-PP, OO-PP-EN2, and OO-pCCD with respect to OO-DOCI plotted logarithmically. OO-PP-EN2 is above OO-DOCI until $R_{\text{H-H}} = 3.2 a_0$ where it goes below and overcorrelates the rest of the way to dissociation. OO-pCCD always overcorrelates relative to OO-DOCI.

TABLE III. Reduced energies computed at $R_{\text{H-H}} = 2.4 a_0$. Each column represents a set of orbitals, while each row is a method. All results computed in STO-6G.

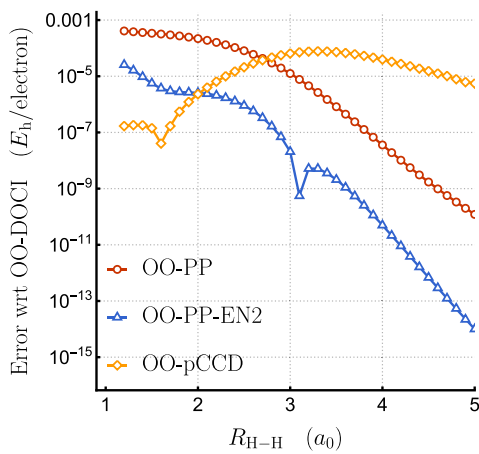
Method	Orbital set		
	PP	pCCD	DOCI
PP	-0.518 56	-0.518 56	-0.518 56
PP-EN2	-0.518 62	-0.518 62	-0.518 62
pCCD	-0.518 63	-0.518 64	-0.518 64
DOCI	-0.518 62	-0.518 62	-0.518 62

than the bonding/antibonding energy splitting. Here, strong correlation is dominant, and pCCD overcorrelates on the order of 0.05 mE_h /electron while the other methods are indiscernible.

Reduced energies for each method at $R_{\text{H-H}} = 2.4 a_0$ are reported in Table III. This point lies halfway between the minimum and the point where strong correlation starts to dominate and thus represents a case where both weak and strong correlation are important. As expected, PP misses weak correlation and is therefore too high. Both EN2 and pCCD are essentially the same as DOCI in all cases.

Reduced energies for H_{10} are shown in Fig. 3, and the results are qualitatively the same as for H_4 . Notice that OO-DOCI is further from FCI than it was for H_4 , as there are more weak correlation effects from the seniority-two and seniority-four sectors. It is again difficult to discern OO-PP, OO-PP-EN2, and OO-pCCD from OO-DOCI, so we plot only the differences in the right panel of Fig. 3.

From the OO-PP solution for H_{10} , the 1-RDM elements and the corresponding VBS gaps are shown in Fig. 4. One sees immediately that the dissociations are smooth, though the bonds are not equivalent but break into a 2-2-1 pattern: the two bonds furthest from the edges of the molecule are equivalent, the two bonds one bond in from the edges are equivalent, and the bond at the center of the molecule is non-degenerate. The VBS gaps decay exponentially with $R_{\text{H-H}}$, consistent with previous observations for RG states.⁹¹ In other words, it is reasonable to consider



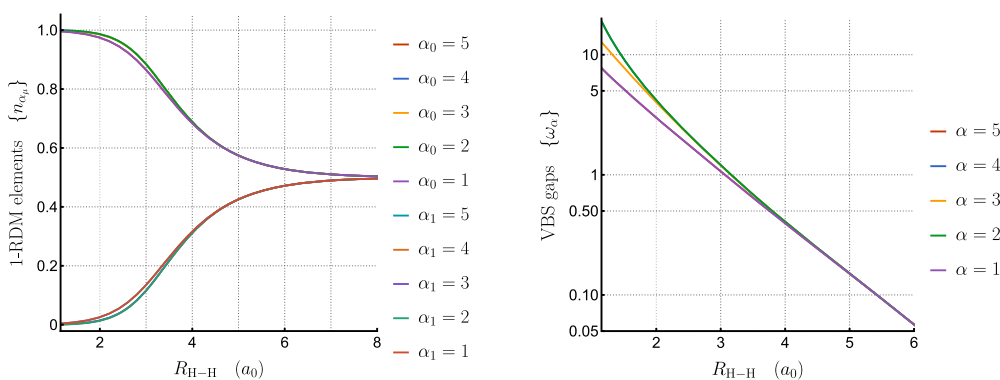


FIG. 4. Symmetric dissociation of H_{10} chain in STO-6G. Left: 1-RDM elements $\{n_\alpha\}$ for H_{10} optimized with OO-PP/STO-6G. Right: VBS gaps $\{\omega_\alpha\}$ for H_{10} optimized with OO-PP/STO-6G plotted logarithmically.



FIG. 5. Progressive dimerization due to Peierls instability of H_{10} : R_0 is kept fixed at $3.6 a_0$ while the distance R is varied.

$$\omega_\alpha = B_\alpha \exp(-A_\alpha R), \quad (46)$$

with only slight deviations at small $R_{\text{H-H}}$. Near equilibrium, the VBS gaps $\{\omega_\alpha\}$ are large, and the pairs of electrons lie principally in the bonding orbital (weak electron correlation). At dissociation, the VBS gaps $\{\omega_\alpha\}$ go to zero, and the occupations of the bonding and antibonding orbitals are equal (strong electron correlation). These two effects are in balance when $\omega_\alpha = 1$, and we have argued previously for RG states that this point marks the transition from weak to strong electron correlation for the particular pair of electrons.⁹¹ For PP, the pair occupation numbers are explicit functions of the VBS gaps, giving the specific value for the bonding orbital occupation as $\frac{1}{2}\left(1 + \frac{1}{\sqrt{2}}\right) \approx 0.8536$.

While equidistant chains of hydrogen atoms are standard tests for strong electron correlation, they are inherently unphysical: at

short distances, these systems do not remain equidistant but spontaneously dimerize into H_2 molecules, a mechanism known as the Peierls instability.¹³⁰ To describe this instability, we consider a system of hydrogen atoms as in Fig. 5. Here, the distances between hydrogen atoms 2 and 3 (and so on) are kept fixed at $R_0 = 3.6 a_0$ while the distance R between hydrogens 1 and 2 is varied. From the numerical results in Fig. 6, it is evident that dimerization stabilizes the energy. OO-DOCI is now a much better treatment at the equilibrium distance, while OO-PP, OO-PP-EN2, and OO-pCCD all deviate smoothly from OO-DOCI. At long distances, OO-DOCI is further from FCI, as the system is trying to dimerize in the opposite manner with individual hydrogen atoms at each end. The curves are parallel, however, and including seniorities two and four would correct the problem.

Finally, OO-PP, OO-PP-EN2, and OO-pCCD were computed for equidistant H_{50} , and the results are shown in Fig. 7. As H_{50} is

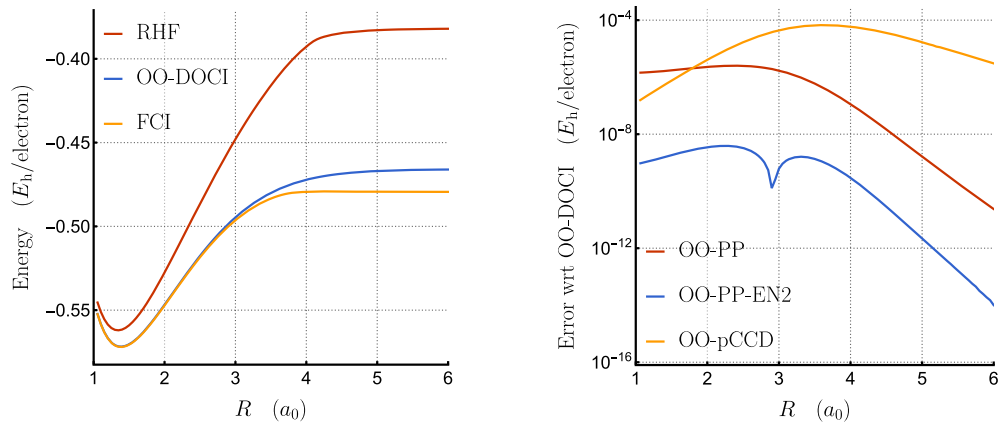


FIG. 6. Progressive dimerization of H_{10} in STO-6G. Left: reduced energies for RHF, OO-DOCI, and FCI. Right: absolute errors of OO-PP, OO-PP-EN2, and OO-pCCD with respect to OO-DOCI plotted logarithmically. OO-PP-EN2 is above OO-DOCI until $R = 2.9 a_0$ where it goes below and overcorrelates the rest of the way to dissociation. OO-pCCD always overcorrelates relative to OO-DOCI.

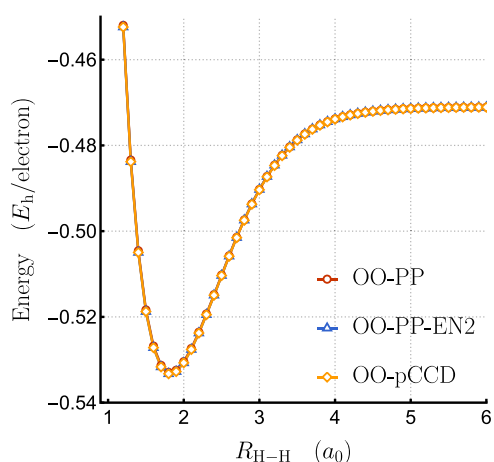


FIG. 7. Symmetric dissociation of H₅₀ chain in STO-6G. Orbitals were optimized separately for PP and pCCD. OO-PP-EN2 is indiscernible from OO-pCCD.

too large for DOCI and FCI, the takeaway is that both OO-PP-EN2 and OO-pCCD remain feasible and give essentially the same result. Rather than plotting the individual 1-RDM elements for H₅₀, we discuss reduced quantities summarizing the physical behavior, known in condensed-matter theory as *order parameters*. One advantage of seeing PP as an eigenvector of Eq. (5), rather than a wavefunction ansatz, is that derived quantities are simple functions of the VBS gaps. First, define the bond order for each VBS as

$$\chi_\alpha = n_{\alpha_0} - n_{\alpha_1} = \frac{\omega_\alpha}{\sqrt{\omega_\alpha^2 + 1}}, \quad (47)$$

half the number of bonding electrons minus the number of antibonding electrons. Here, 0 ≤ χ_α < 1, approaching 1 in the limit of large ω_α. In spin systems, this corresponds to the *magnetization*, from which thermodynamic quantities are computed.¹³¹ Another order parameter, the Jaynes entropy,^{132,133}

$$S_J = - \sum_p n_p \ln n_p, \quad (48)$$

is indicative of strong correlation in bond-breaking processes.^{134–136} However, the Jaynes entropy gives *no* description of weak correlation,¹³⁷ as occupation numbers close to 0 or 1 give vanishing contributions in Eq. (48). For PP, the Jaynes entropy simplifies to a sum of individual contributions from each VBS,

$$S_\alpha = \ln 2 - \sum_{n=1}^{\infty} \frac{\chi_\alpha^{2n}}{2n(2n-1)}, \quad (49)$$

in terms of the bond order. Since |χ_α| < 1, this series always converges.

Finally, the off-diagonal long-range order (ODLRO),^{138–140} defined as

$$\Delta_{OD} = \frac{2}{N} \sum_{pq} P_{pq} = 1 - \frac{2}{N} \sum_\alpha \frac{1}{\sqrt{\omega_\alpha^2 + 1}}, \quad (50)$$

is an order parameter describing systems dominated by pairing interactions. Usually, ODLRO is computed for attractive systems,

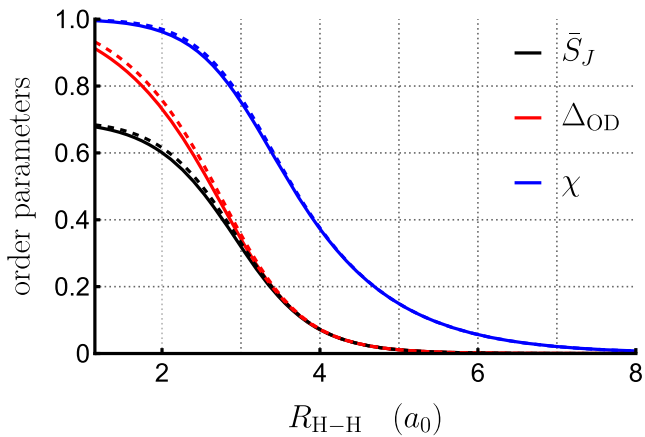


FIG. 8. Order parameters in the symmetric dissociation of equidistant H₁₀ (solid lines) and H₅₀ (dashed lines) chains in STO-6G, computed from the OO-PP RDM elements.

where it identifies an eigenvalue of *P* that scales with the size of the system, indicating *long-range order*.^{141–144} In bond-breaking processes, the pairing is repulsive, and ODLRO sharply goes to zero as seen in Fig. 8. The name is less descriptive here, but the order parameter still captures the transition in behavior.

To demonstrate that these three order parameters contain the same information, we plot

$$\chi = \frac{2}{N} \sum_\alpha \chi_\alpha, \quad (51)$$

$$\bar{S}_J = -\frac{2}{N} S_J + \ln 2, \quad (52)$$

and Δ_{OD} for linear equidistant H₁₀ and H₅₀ in Fig. 8. One immediately notices that the three order parameters are qualitatively the same and nearly sigmoidal in shape. Δ_{OD} will eventually level out to 1 as the individual ω_α become large. The three order parameters are essentially invariant to size, with minor variations as the bonds in linear hydrogen chains are not all equivalent. Of the three, the bond order is to be preferred, as it is the most direct to compute, and is most familiar to chemists.

We will close with an intuitive interpretation from the bond order. As a function of ω_α, the bond order χ_α is strictly concave, but as a function of *R*, there is clearly an inflection point. It is reasonable to interpret the inflection point as where the bond breaks.¹⁴⁵ In Ref. 145, the authors note that this point is usually incredibly difficult to compute, as it would require an FCI wavefunction, and instead consider the maximum of the polarizability along the bond axis as the point where the bond breaks. One can, however, easily calculate this point for PP, using

$$\frac{\partial^2 \chi_\alpha}{\partial R^2} = \frac{\partial^2 \chi_\alpha}{\partial \omega_\alpha^2} \left(\frac{\partial \omega_\alpha}{\partial R} \right)^2 + \frac{\partial \chi_\alpha}{\partial \omega_\alpha} \frac{\partial^2 \omega_\alpha}{\partial R^2}, \quad (53)$$

with the parametrization (46) giving

$$\frac{1}{A_\alpha^2} (\omega_\alpha^2 + 1)^{\frac{5}{2}} \frac{\partial^2 \chi_\alpha}{\partial R^2} = \omega_\alpha (1 - 2\omega_\alpha^2), \quad (54)$$

and thus a solution of $\omega_\alpha = \frac{1}{\sqrt{2}}$. This corresponds to a bond order of $\chi_\alpha = \frac{1}{\sqrt{3}} \approx 0.5774$, or a bonding orbital occupation of $n_{\alpha_0} \approx 0.7887$. These are ideal values; inclusion of weak correlation will decrease them slightly. From Fig. 4, it is clear that parametrization (46) is not perfect but it is only needed in the neighborhood of the inflection point. For H₂ in the minimal basis STO-6G, OO-PP predicts bond breaking near $R \approx 3.335a_0$, close to the value $R = 1.75 \text{ \AA} \approx 3.307a_0$ obtained in Ref. 145 from the polarizability (FCI/aug-cc-pVTZ).

IV. CONCLUSION

We have demonstrated that the PP wavefunction, long recognized as a key model for strong correlation, naturally emerges as an eigenvector of a simplified reduced BCS Hamiltonian formulated in the space of bonding and antibonding orbitals. This construction clarifies the formal relationship between PP, pCCD, and RG states, establishing a unifying framework that connects orbital- and geminal-based descriptions of electron correlation. Within this picture, the complementary eigenvectors of the simplified Hamiltonian provide a systematic route to include weak correlation effects through perturbative corrections. In particular, EN2 built upon PP yields results nearly indistinguishable from pCCD, confirming that the latter effectively incorporates the same physical content through a CC parameterization. Because PP is derived from a well-defined model Hamiltonian, one can explicitly construct a complete Hilbert space in which corrections may be introduced systematically, much like in single-reference methods for weakly correlated systems. While the present treatment is restricted to the seniority-zero sector, including the PP limit to RG states with non-zero seniority^{118,119} is a tedious but straightforward exercise. In contrast, pCCD lacks a systematic correction scheme capable of seamlessly incorporating both weak and strong correlation.^{74,77,78,111,146–149}

ACKNOWLEDGMENTS

P.A.J. thanks the Natural Sciences and Engineering Research Council of Canada (Grant No. RGPIN-2024-05610) for funding. This research was made possible in part by the Digital Research Alliance of Canada. P.-F.L. thanks the European Research Council (ERC) under the European Union's Horizon 2020 research and innovation program (Grant Agreement No. 863481) for funding.

AUTHOR DECLARATIONS

Conflict of Interest

The authors have no conflicts to disclose.

Author Contributions

Paul A. Johnson: Conceptualization (equal); Data curation (equal); Formal analysis (equal); Funding acquisition (equal); Supervision (equal); Writing – original draft (equal); Writing – review & editing (equal). **Charles-Émile Fecteau:** Data curation (supporting). **Samuel Nadeau:** Data curation (supporting). **Mauricio Rodríguez-Mayorga:** Data curation (supporting); Writing – review & editing (supporting). **Pierre-François Loos:** Conceptualization

(equal); Data curation (equal); Formal analysis (equal); Funding acquisition (equal); Supervision (equal); Writing – original draft (equal); Writing – review & editing (equal).

DATA AVAILABILITY

The data that support the findings of this study are available within the article.

APPENDIX: PP-EN2 EXPRESSIONS

1. RDM elements

RDM elements for the intra-pair excitation $|\Psi_\alpha^\alpha\rangle$ are almost the same as for $|\Psi\rangle$. The only difference for the 1-RDM occurs in the VBS, which has been modified:

$$(n_{\alpha_\mu})_\alpha^\alpha = \frac{1}{2} \left[1 - \frac{(-1)^\mu \omega_\alpha}{\sqrt{\omega_\alpha^2 + 1}} \right] = n_{\alpha_{1-\mu}}, \quad (\text{A1})$$

while the pair-transfer element in the modified VBS becomes

$$(P_{\alpha_0 \alpha_1})_\alpha^\alpha = (P_{\alpha_1 \alpha_0})_\alpha^\alpha = +\sqrt{(n_{\alpha_0})_\alpha^\alpha (n_{\alpha_1})_\alpha^\alpha} = -P_{\alpha_0 \alpha_1}. \quad (\text{A2})$$

Symbolically, the density–density elements do not change at all; they remain the product of the 1-RDM elements (which are themselves modified), as in Eq. (11).

RDM elements for the inter-pair excitations $|\Psi_\alpha^\beta\rangle$ are also simple modifications of those for $|\Psi\rangle$. In particular, the α th VBS is now empty, while the β th VBS is full. As a result, the 1-RDM elements are integers, that is,

$$(n_{\alpha_0})_\alpha^\beta = (n_{\alpha_1})_\alpha^\beta = 0, \quad (\text{A3a})$$

$$(n_{\beta_0})_\alpha^\beta = (n_{\beta_1})_\alpha^\beta = 1, \quad (\text{A3b})$$

while pair-transfer is not possible in either the empty or the full VBS:

$$(P_{\alpha_0 \alpha_1})_\alpha^\beta = (P_{\alpha_1 \alpha_0})_\alpha^\beta = (P_{\beta_0 \beta_1})_\alpha^\beta = (P_{\beta_1 \beta_0})_\alpha^\beta = 0. \quad (\text{A4})$$

Again, the density–density elements are the product of the individual 1-RDM elements, as in Eq. (11), with the additional element:

$$(D_{\beta_0 \beta_1})_\alpha^\beta = 1. \quad (\text{A5})$$

RDM elements for the double pair excitation $|\Psi_{\alpha\beta}^{\alpha\beta}\rangle$ are the same as Eqs. (A1) and (A2) but in both the α th and β th VBS. Again, the density–density elements do not change symbolically.

2. Energy denominators

To compute the energy denominators, the primitive objects are those for the intra-pair excitations:

$$\begin{aligned} (\omega_\alpha^2 + 1)^{\frac{1}{2}} (E^{(0)} - E_\alpha^\alpha) &= -2L_{\alpha_0 \alpha_1} + 2\omega_\alpha \sum_\mu (-1)^\mu \left(h_{\alpha_\mu \alpha_\mu} + \frac{1}{2} L_{\alpha_\mu \alpha_\mu} \right. \\ &\quad \left. + \sum_{\beta(\neq \alpha)} \sum_v G_{\alpha_\mu \beta_v} n_{\beta_v} \right), \end{aligned} \quad (\text{A6})$$

which, because of the stationarity of the energy with respect to the energy gaps ω_α [see Eq. (17)], reduces to

$$E^{(0)} - E_\alpha^\alpha = \frac{L_{\alpha_0\alpha_1}}{P_{\alpha_0\alpha_1}}. \quad (\text{A7})$$

Energy denominators for double pair excitations are obtained as an update:

$$\begin{aligned} E^{(0)} - E_{\alpha\beta}^{\alpha\beta} &= \frac{L_{\alpha_0\alpha_1}}{P_{\alpha_0\alpha_1}} + \frac{L_{\beta_0\beta_1}}{P_{\beta_0\beta_1}} - 2(n_{\alpha_1} - n_{\alpha_0})(n_{\beta_1} - n_{\beta_0}) \\ &\times \sum_{\mu\nu} (-1)^{\mu+\nu} G_{\alpha_\mu\beta_\nu}. \end{aligned} \quad (\text{A8})$$

With the electronic Hessian (16), this may also be written as

$$\begin{aligned} E^{(0)} - E_{\alpha\beta}^{\alpha\beta} &= -2(\omega_\alpha^2 + 1)^2 \frac{\partial^2 E}{\partial \omega_\alpha^2} - 2(\omega_\beta^2 + 1)^2 \frac{\partial^2 E}{\partial \omega_\beta^2} \\ &- 4\omega_\alpha\omega_\beta(\omega_\alpha^2 + 1)(\omega_\beta^2 + 1) \frac{\partial^2 E}{\partial \omega_\alpha \partial \omega_\beta}. \end{aligned} \quad (\text{A9})$$

The energy denominators for the inter-pair excitations are likewise an update of the intra-pair excitations,

$$\begin{aligned} E^{(0)} - E_\alpha^\beta &= \frac{L_{\alpha_0\alpha_1}}{2P_{\alpha_0\alpha_1}} + \frac{L_{\beta_0\beta_1}}{2P_{\beta_0\beta_1}} + \varepsilon_{\alpha_0} + \varepsilon_{\alpha_1} - \varepsilon_{\beta_0} - \varepsilon_{\beta_1} - 2G_{\beta_0\beta_1} \\ &+ 2 \sum_{\mu\nu} G_{\alpha_\mu\beta_\nu} n_{\alpha_\mu} n_{\beta_{1-\nu}}, \end{aligned} \quad (\text{A10})$$

where ε are the orbital energies defined in Eq. (18).

3. Transition elements

Energy numerators require transition density matrix (TDM) elements from the reference wavefunction $|\Psi\rangle$ to its excited states. The intra-pair excitation $|\Psi_\alpha^\alpha\rangle$ only couples to the reference through elements involving the α th VBS. The normalized non-zero one-body elements are

$$\langle\Psi_\alpha^\alpha|\hat{n}_{\alpha_0}|\Psi\rangle = -\langle\Psi_\alpha^\alpha|\hat{n}_{\alpha_1}|\Psi\rangle = -P_{\alpha_0\alpha_1}, \quad (\text{A11})$$

which evidently sum to zero. There are also non-zero pair-transfer elements in the α th VBS, which, when normalized, become

$$\langle\Psi_\alpha^\alpha|\hat{P}_{\alpha_1}^+\hat{P}_{\alpha_0}^-|\Psi\rangle = n_{\alpha_0}, \quad (\text{A12a})$$

$$\langle\Psi_\alpha^\alpha|\hat{P}_{\alpha_0}^+\hat{P}_{\alpha_1}^-|\Psi\rangle = -n_{\alpha_1}. \quad (\text{A12b})$$

Notice that pair-transfer TDM elements are *not* symmetric. Non-zero density-density elements only occur when one index is in the α th VBS and the other is not. When normalized, we have

$$\langle\Psi_\alpha^\alpha|\hat{n}_{\alpha_0}\hat{n}_{\beta_1}|\Psi\rangle = -\langle\Psi_\alpha^\alpha|\hat{n}_{\alpha_1}\hat{n}_{\beta_0}|\Psi\rangle = \langle\Psi_\alpha^\alpha|\hat{n}_{\alpha_0}|\Psi\rangle n_{\beta_1}, \quad (\text{A13})$$

where, on the right-hand side, the 1-RDM elements $(n_{\beta_1})_\alpha^\alpha = n_{\beta_1}$ are identical as β_1 is not in the α th VBS.

The double-pair excitation $|\Psi_{\alpha\beta}^{\alpha\beta}\rangle$ couples to the reference $|\Psi\rangle$ only through the normalized elements:

$$\begin{aligned} \langle\Psi_{\alpha\beta}^{\alpha\beta}|\hat{n}_{\alpha_0}\hat{n}_{\beta_0}|\Psi\rangle &= -\langle\Psi_{\alpha\beta}^{\alpha\beta}|\hat{n}_{\alpha_0}\hat{n}_{\beta_1}|\Psi\rangle = -\langle\Psi_{\alpha\beta}^{\alpha\beta}|\hat{n}_{\alpha_1}\hat{n}_{\beta_0}|\Psi\rangle \\ &= \langle\Psi_{\alpha\beta}^{\alpha\beta}|\hat{n}_{\alpha_1}\hat{n}_{\beta_1}|\Psi\rangle = P_{\alpha_0\alpha_1}P_{\beta_0\beta_1}. \end{aligned} \quad (\text{A14})$$

Any state with more than two pair excitations will not couple to the reference $|\Psi\rangle$ through a two-electron operator.

The inter-pair excitation $|\Psi_\alpha^\beta\rangle$ only couples to $|\Psi\rangle$ through pair transfers taking a pair of electrons from the α th VBS and placing it in the β th. The non-zero normalized elements are

$$\langle\Psi_\alpha^\beta|\hat{P}_{\beta_{1-\nu}}^+\hat{P}_{\alpha_\mu}^-|\Psi\rangle = (-1)^{\mu+\nu} \sqrt{n_{\alpha_\mu} n_{\beta_\nu}}. \quad (\text{A15})$$

Again, pair-transfer TDM elements are not symmetric and are forbidden in the reverse processes:

$$\begin{aligned} \langle\Psi_\alpha^\beta|\hat{P}_{\alpha_0}^+\hat{P}_{\beta_0}^-|\Psi\rangle &= \langle\Psi_\alpha^\beta|\hat{P}_{\alpha_1}^+\hat{P}_{\beta_0}^-|\Psi\rangle = \langle\Psi_\alpha^\beta|\hat{P}_{\alpha_0}^+\hat{P}_{\beta_1}^-|\Psi\rangle \\ &= \langle\Psi_\alpha^\beta|\hat{P}_{\alpha_1}^+\hat{P}_{\beta_1}^-|\Psi\rangle = 0. \end{aligned} \quad (\text{A16})$$

The energy numerators are thus simple to evaluate, giving

$$\begin{aligned} (\omega_\alpha^2 + 1)^{\frac{1}{2}} \langle\Psi_\alpha^\alpha|\hat{H}_C|\Psi\rangle &= \omega_\alpha L_{\alpha_0\alpha_1} + \sum_\mu (-1)^\mu \left(h_{\alpha_\mu\alpha_\mu} + \frac{1}{2} L_{\alpha_\mu\alpha_\mu} \right. \\ &\quad \left. + \sum_{\beta(\neq\alpha)} \sum_\nu G_{\alpha_\mu\beta_\nu} n_{\beta_\nu} \right), \end{aligned} \quad (\text{A17})$$

which *vanishes* as a consequence of the stationarity of the energy given by Eq. (17). The intra-pair transfers thus give no contribution, analogous to the Brillouin theorem for Slater determinants in the HF orbitals. The energy numerators for the double-pair excitations are

$$\langle\Psi_{\alpha\beta}^{\alpha\beta}|\hat{H}_C|\Psi\rangle = 2P_{\alpha_0\alpha_1}P_{\beta_0\beta_1} \sum_{\mu\nu} (-1)^{\mu+\nu} G_{\alpha_\mu\beta_\nu}, \quad (\text{A18})$$

or, from Eq. (16), we have

$$\langle\Psi_{\alpha\beta}^{\alpha\beta}|\hat{H}_C|\Psi\rangle = 2(\omega_\alpha^2 + 1)(\omega_\beta^2 + 1) \frac{\partial^2 E}{\partial \omega_\alpha \partial \omega_\beta}. \quad (\text{A19})$$

For the inter-pair excitations, the energy numerators are likewise simple:

$$\begin{aligned} \langle\Psi_\alpha^\beta|\hat{H}_C|\Psi\rangle &= L_{\beta_1\alpha_0}\sqrt{n_{\alpha_0} n_{\beta_0}} - L_{\beta_1\alpha_1}\sqrt{n_{\alpha_1} n_{\beta_0}} \\ &\quad - L_{\beta_0\alpha_0}\sqrt{n_{\alpha_0} n_{\beta_1}} + L_{\beta_0\alpha_1}\sqrt{n_{\alpha_1} n_{\beta_1}}. \end{aligned} \quad (\text{A20})$$

REFERENCES

- T. Helgaker, P. Jørgensen, and J. Olsen, *Molecular Electronic-Structure Theory* (Wiley & Sons, West Sussex, 2000).
- I. Shavitt and R. J. Bartlett, *Many-Body Methods in Chemistry and Physics* (Cambridge University Press, Cambridge, 2009).
- P. A. M. Dirac and N. H. D. Bohr, "The quantum theory of the emission and absorption of radiation," *Proc. R. Soc. London, Ser. A* **114**, 243–265 (1927).
- P. Jørgensen and J. Simons, *Second Quantization-based Methods in Quantum Chemistry* (Elsevier, 1981).
- G. C. Wick, "The evaluation of the collision matrix," *Phys. Rev.* **80**, 268–272 (1950).

- ⁶T. D. Crawford and H. F. Schaefer, "An introduction to coupled cluster theory for computational chemists," in *Reviews in Computational Chemistry* (John Wiley & Sons, Ltd, Chichester, England, 2000), pp. 33–136.
- ⁷S. Hirata, "Tensor contraction engine: Abstraction and automated parallel implementation of configuration-interaction, coupled-cluster, and many-body perturbation theories," *J. Phys. Chem. A* **107**, 9887–9897 (2003).
- ⁸N. C. Rubin and A. E. DePrince III, "p[†]q: A tool for prototyping many-body methods for quantum chemistry," *Mol. Phys.* **119**, e1954709 (2021).
- ⁹F. A. Evangelista, "Automatic derivation of many-body theories based on general Fermi vacua," *J. Chem. Phys.* **157**, 064111 (2022).
- ¹⁰R. Quintero-Monsebaiz and P.-F. Loos, "Equation generator for equation-of-motion coupled cluster assisted by computer algebra system," *AIP Adv.* **13**, 085035 (2023).
- ¹¹M. D. Liebenthal, S. H. Yuwono, L. N. Koulias, R. R. Li, N. C. Rubin, and A. E. DePrince III, "Automated quantum chemistry code generation with the p[†]q package," *J. Phys. Chem. A* **129**, 6679–6693 (2025).
- ¹²B. O. Roos, P. R. Taylor, and P. E. M. Sigbahn, "A complete active space SCF method (CASSCF) using a density matrix formulated super-CI approach," *Chem. Phys.* **48**, 157 (1980).
- ¹³B. O. Roos, "The complete active space SCF method in a Fock-matrix-based super-CI formulation," *Int. J. Quantum Chem.* **18**, 175–189 (2009).
- ¹⁴B. O. Roos, "Multiconfigurational quantum chemistry," in *Theory and Applications of Computational Chemistry* (Elsevier, 2005), pp. 725–764.
- ¹⁵S. R. White, "Density matrix formulation for quantum renormalization groups," *Phys. Rev. Lett.* **69**, 2863 (1992).
- ¹⁶S. R. White, "Density-matrix algorithms for quantum renormalization groups," *Phys. Rev. B* **48**, 10345 (1993).
- ¹⁷G. K.-L. Chan and S. Sharma, "The density matrix renormalization group in quantum chemistry," *Annu. Rev. Phys. Chem.* **62**, 465–481 (2011).
- ¹⁸S. Wouters and D. Van Neck, "The density matrix renormalization group for ab initio quantum chemistry," *Eur. Phys. J. D* **68**, 272 (2014).
- ¹⁹S. Szalay, M. Pfeffer, V. Murg, G. Barcza, F. Verstraete, R. Schneider, and Ö. Legeza, "Tensor product methods and entanglement optimization for *ab initio* quantum chemistry," *Int. J. Quantum Chem.* **115**, 1342–1391 (2015).
- ²⁰A. Baiardi and M. Reiher, "The density matrix renormalization group in chemistry and molecular physics: Recent developments and new challenges," *J. Chem. Phys.* **152**, 040903 (2020).
- ²¹N. Oliphant and L. Adamowicz, "Coupled-cluster method truncated at quadruples," *J. Chem. Phys.* **95**, 6645 (1991).
- ²²S. A. Kucharski and R. J. Bartlett, "The coupled-cluster single, double, triple, and quadruple excitation method," *J. Chem. Phys.* **97**, 4282 (1992).
- ²³B. Huron, J. P. Malrieu, and P. Rancurel, "Iterative perturbation calculations of ground and excited state energies from multiconfigurational zeroth-order wavefunctions," *J. Chem. Phys.* **58**, 5745 (1973).
- ²⁴E. Giner, A. Scemama, and M. Caffarel, "Using perturbatively selected configuration interaction in quantum Monte Carlo calculations," *Can. J. Chem.* **91**, 879 (2013).
- ²⁵X. Liu and J. E. Subotnik, "The variationally orbital-adapted configuration interaction singles (VOA-CIS) approach to electronically excited states," *J. Chem. Theory Comput.* **10**, 1004 (2014).
- ²⁶J. B. Schriber and F. A. Evangelista, "Communication: An adaptive configuration interaction approach for strongly correlated electrons with tunable accuracy," *J. Chem. Phys.* **144**, 161106 (2016).
- ²⁷A. A. Holmes, N. M. Tubman, and C. J. Umrigar, "Heat-bath configuration interaction: An efficient selected configuration interaction algorithm inspired by heat-bath sampling," *J. Chem. Theory Comput.* **12**, 3674 (2016).
- ²⁸Y. Garniron, A. Scemama, E. Giner, M. Caffarel, and P. F. Loos, "Selected configuration interaction dressed by perturbation," *J. Chem. Phys.* **149**, 064103 (2018).
- ²⁹A. C. Hurley, J. E. Lennard-Jones, and J. A. Pople, "The molecular orbital theory of chemical valency XVI. A theory of paired-electrons in polyatomic molecules," *Proc. R. Soc. London, Ser. A* **220**, 446–455 (1953).
- ³⁰H. Shull, "Natural spin orbital analysis of hydrogen molecule wave functions," *J. Chem. Phys.* **30**, 1405–1413 (1959).
- ³¹T. L. Allen and H. Shull, "The chemical bond in molecular quantum mechanics," *J. Chem. Phys.* **35**, 1644–1651 (1961).
- ³²A. J. Coleman, "Structure of fermion density matrices," *Rev. Mod. Phys.* **35**, 668–686 (1963).
- ³³G. N. Lewis, "The atom and the molecule," *J. Am. Chem. Soc.* **38**, 762–785 (1916).
- ³⁴P. R. Surján, *An Introduction to the Theory of Geminals* (Springer, Berlin, 1999).
- ³⁵A. J. Coleman, "Structure of fermion density matrices. II. Antisymmetrized geminal powers," *J. Math. Phys.* **6**, 1425–1431 (1965).
- ³⁶D. M. Silver, "Natural orbital expansion of interacting geminals," *J. Chem. Phys.* **50**, 5108–5116 (1969).
- ³⁷P. A. Limacher, P. W. Ayers, P. A. Johnson, S. De Baerdemacker, D. Van Neck, and P. Bultinck, "A new mean-field method suitable for strongly correlated electrons: Computationally facile antisymmetric products of nonorthogonal geminals," *J. Chem. Theory Comput.* **9**, 1394–1401 (2013).
- ³⁸P. Tecmer, K. Boguslawski, P. A. Johnson, P. A. Limacher, M. Chan, T. Verstraeten, and P. W. Ayers, "Assessing the accuracy of new geminal-based approaches," *J. Phys. Chem. A* **118**, 9058–9068 (2014).
- ³⁹P. A. Johnson, C.-É. Fecteau, F. Berthiaume, S. Cloutier, L. Carrier, M. Gratton, P. Bultinck, S. De Baerdemacker, D. Van Neck, P. Limacher, and P. W. Ayers, "Richardson–Gaudin mean-field for strong correlation in quantum chemistry," *J. Chem. Phys.* **153**, 104110 (2020).
- ⁴⁰S. De Baerdemacker and D. Van Neck, "Geminal theory within the seniority formalism and bi-variational principle," in *Novel Treatments of Strong Correlations, Advances in Quantum Chemistry*, edited by R. A. M. Quintana and J. F. Stanton (Academic Press, 2024), Vol. 90, pp. 185–218.
- ⁴¹J. Cullen, "Generalized valence bond solutions from a constrained coupled cluster method," *Chem. Phys.* **202**, 217–229 (1996).
- ⁴²T. Thorsteinsson, D. L. Cooper, J. Gerratt, P. B. Karadakov, and M. Raimondi, "Modern valence bond representations of CASSCF wavefunctions," *Theor. Chim. Acta* **93**, 343–366 (1996).
- ⁴³T. Thorsteinsson and D. L. Cooper, "Exact transformations of CI spaces, VB representations of CASSCF wavefunctions and the optimization of VB wavefunctions," *Theor. Chim. Acta* **94**, 233–245 (1996).
- ⁴⁴T. Thorsteinsson, D. L. Cooper, J. Gerratt, and M. Raimondi, "Symmetry adaptation and the utilization of point group symmetry in valence bond calculations, including CASVB," *Theor. Chim. Acta* **95**, 131–150 (1997).
- ⁴⁵H. R. Larsson, C. A. Jiménez-Hoyos, and G. K.-L. Chan, "Minimal matrix product states and generalizations of mean-field and geminal wave functions," *J. Chem. Theory Comput.* **16**, 5057–5066 (2020).
- ⁴⁶T. H. Dunning, Jr., L. T. Xu, T. Y. Takeshita, and B. A. Lindquist, "Insights into the electronic structure of molecules from generalized valence bond theory," *J. Phys. Chem. A* **120**, 1763–1778 (2016).
- ⁴⁷L. Bytautas, T. M. Henderson, C. A. Jimenez-Hoyos, J. K. Ellis, and G. E. Scuseria, "Seniority and orbital symmetry as tools for establishing a full configuration interaction hierarchy," *J. Chem. Phys.* **135**, 044119 (2011).
- ⁴⁸D. W. Smith and S. J. Fogel, "Natural orbitals and geminals of the beryllium atom," *J. Chem. Phys.* **43**, S91–S96 (1965).
- ⁴⁹A. Veillard and E. Clementi, "Complete multi-configuration self-consistent field theory," *Theor. Chim. Acta* **7**, 133–143 (1967).
- ⁵⁰L. Bytautas, G. E. Scuseria, and K. Ruedenberg, "Seniority number description of potential energy surfaces: Symmetric dissociation of water, N₂, C₂, and Be₂," *J. Chem. Phys.* **143**, 094105 (2015).
- ⁵¹D. R. Alcoba, A. Torre, L. Lain, G. E. Massaccesi, and O. B. Oña, "Configuration interaction wave functions: A seniority number approach," *J. Chem. Phys.* **140**, 234103 (2014).
- ⁵²D. R. Alcoba, A. Torre, L. Lain, O. B. Oña, P. Capuzzi, M. Van Raemdonck, P. Bultinck, and D. Van Neck, "A hybrid configuration interaction treatment based on seniority number and excitation schemes," *J. Chem. Phys.* **141**, 244118 (2014).
- ⁵³F. Koskoski, Y. Damour, and P.-F. Loos, "Hierarchy configuration interaction: Combining seniority number and excitation degree," *J. Phys. Chem. Lett.* **13**, 4342–4349 (2022).
- ⁵⁴F. Koskoski and P.-F. Loos, "Seniority and hierarchy configuration interaction for radicals and excited states," *J. Chem. Theory Comput.* **19**, 8654–8670 (2023).

- ⁵⁵T. Stein, T. M. Henderson, and G. E. Scuseria, "Seniority zero pair coupled cluster doubles theory," *J. Chem. Phys.* **140**, 214113 (2014).
- ⁵⁶T. M. Henderson, I. W. Bulik, T. Stein, and G. E. Scuseria, "Seniority-based coupled cluster theory," *J. Chem. Phys.* **141**, 244104 (2014).
- ⁵⁷K. Boguslawski, P. Tecmer, P. W. Ayers, P. Bultinck, S. De Baerdemacker, and D. Van Neck, "Efficient description of strongly correlated electrons with mean-field cost," *Phys. Rev. B* **89**, 201106(R) (2014).
- ⁵⁸K. Boguslawski, P. Tecmer, P. Bultinck, S. De Baerdemacker, D. Van Neck, and P. W. Ayers, "Nonvariational orbital optimization techniques for the AP1roG wave function," *J. Chem. Theory Comput.* **10**, 4873–4882 (2014).
- ⁵⁹K. Boguslawski, P. Tecmer, P. A. Limacher, P. A. Johnson, P. W. Ayers, P. Bultinck, S. De Baerdemacker, and D. Van Neck, "Projected seniority-two orbital optimization of the antisymmetric product of one-reference orbital geminal," *J. Chem. Phys.* **140**, 214114 (2014).
- ⁶⁰K. Boguslawski, P. Tecmer, and Ö. Legeza, "Analysis of two-orbital correlations in wave functions restricted to electron-pair states," *Phys. Rev. B* **94**, 155126 (2016).
- ⁶¹F. Kossoski, A. Marie, A. Scemama, M. Caffarel, and P.-F. Loos, "Excited states from state-specific orbital-optimized pair coupled cluster," *J. Chem. Theory Comput.* **17**, 4756–4768 (2021).
- ⁶²A. Marie, F. Kossoski, and P.-F. Loos, "Variational coupled cluster for ground and excited states," *J. Chem. Phys.* **155**, 104105 (2021).
- ⁶³P. A. Limacher, T. D. Kim, P. W. Ayers, P. A. Johnson, S. De Baerdemacker, D. Van Neck, and P. Bultinck, "The influence of orbital rotation on the energy of closed-shell wavefunctions," *Mol. Phys.* **112**, 853–862 (2014).
- ⁶⁴W. A. Goddard III, "Improved quantum theory of many-electron systems. II. The basic method," *Phys. Rev.* **157**, 81 (1967).
- ⁶⁵W. J. Hunt, P. J. Hay, and W. A. Goddard III, "Self-consistent procedures for generalized valence bond wavefunctions. Applications H₃, BH, H₂O, C₂H₆, and O₂," *J. Chem. Phys.* **57**, 738–748 (1972).
- ⁶⁶P. J. Hay, W. J. Hunt, and W. A. Goddard III, "Generalized valence bond description of simple alkanes, ethylene, and acetylene," *J. Am. Chem. Soc.* **94**, 8293–8301 (1972).
- ⁶⁷W. A. Goddard III, T. H. Dunning, W. J. Hunt, and P. J. Hay, "Generalized valence bond description of bonding in low-lying states of molecules," *Acc. Chem. Res.* **6**, 368–376 (1973).
- ⁶⁸F. W. Bobrowicz and W. A. Goddard, "The self-consistent field equations for generalized valence bond and open-shell Hartree-Fock wave functions," in *Methods of Electronic Structure Theory*, edited by H. F. Schaefer (Springer US, Boston, MA, 1977), pp. 79–127.
- ⁶⁹W. A. Goddard III and L. B. Harding, "The description of chemical bonding from ab initio calculations," *Annu. Rev. Phys. Chem.* **29**, 363–396 (1978).
- ⁷⁰C. E. Dykstra, "Perfect pairing valence bond generalization of self-consistent electron pair theory," *J. Chem. Phys.* **72**, 2928–2935 (1980).
- ⁷¹D. W. Small and M. Head-Gordon, "Tractable spin-pure methods for bond breaking: Local many-electron spin-vector sets and an approximate valence bond model," *J. Chem. Phys.* **130**, 084103 (2009).
- ⁷²K. V. Lawler, D. W. Small, and M. Head-Gordon, "Orbitals that are unrestricted in active pairs for generalized valence bond coupled cluster methods," *J. Phys. Chem. A* **114**, 2930–2938 (2010).
- ⁷³D. W. Small and M. Head-Gordon, "Post-modern valence bond theory for strongly correlated electron spins," *Phys. Chem. Chem. Phys.* **13**, 19285–19297 (2011).
- ⁷⁴S. Lehtola, J. Parkhill, and M. Head-Gordon, "Cost-effective description of strong correlation: Efficient implementations of the perfect quadruples and perfect hexuples models," *J. Chem. Phys.* **145**, 134110 (2016).
- ⁷⁵G. J. O. Beran, B. Austin, A. Sodt, and M. Head-Gordon, "Unrestricted perfect pairing: The simplest wave-function-based model chemistry beyond mean field," *J. Phys. Chem. A* **109**, 9183–9192 (2005).
- ⁷⁶G. J. O. Beran, M. Head-Gordon, and S. R. Gwaltney, "Second-order correction to perfect pairing: An inexpensive electronic structure method for the treatment of strong electron-electron correlations," *J. Chem. Phys.* **124**, 114107 (2006).
- ⁷⁷J. A. Parkhill, K. Lawler, and M. Head-Gordon, "The perfect quadruples model for electron correlation in a valence active space," *J. Chem. Phys.* **130**, 084101 (2009).
- ⁷⁸J. A. Parkhill and M. Head-Gordon, "A tractable and accurate electronic structure method for static correlations: The perfect hexuples model," *J. Chem. Phys.* **133**, 024103 (2010).
- ⁷⁹J. A. Parkhill and M. Head-Gordon, "A truncation hierarchy of coupled cluster models of strongly correlated systems based on perfect-pairing references: The singles+doubles models," *J. Chem. Phys.* **133**, 124102 (2010).
- ⁸⁰J. Cullen, "Is GVB-CI superior to CASSCF?," *J. Comput. Chem.* **20**, 999–1008 (1999).
- ⁸¹T. V. Voorhis and M. Head-Gordon, "A nonorthogonal approach to perfect pairing," *J. Chem. Phys.* **112**, 5633–5638 (2000).
- ⁸²T. Van Voorhis and M. Head-Gordon, "The imperfect pairing approximation," *Chem. Phys. Lett.* **317**, 575–580 (2000).
- ⁸³T. Van Voorhis and M. Head-Gordon, "Connections between coupled cluster and generalized valence bond theories," *J. Chem. Phys.* **115**, 7814–7821 (2001).
- ⁸⁴D. W. Small and M. Head-Gordon, "A fusion of the closed-shell coupled cluster singles and doubles method and valence-bond theory for bond breaking," *J. Chem. Phys.* **137**, 114103 (2012).
- ⁸⁵J. Cullen, "An approximate diatomics in molecules formulation of generalized valence bond theory," *J. Comput. Chem.* **29**, 497–504 (2008).
- ⁸⁶J. S. Kottmann and A. Aspuru-Guzik, "Optimized low-depth quantum circuits for molecular electronic structure using a separable-pair approximation," *Phys. Rev. A* **105**, 032449 (2022).
- ⁸⁷J. S. Kottmann, "Molecular quantum circuit design: A graph-based approach," *Quantum* **7**, 1073 (2023).
- ⁸⁸J. S. Kottmann and F. Scala, "Quantum algorithmic approach to multiconfigurational valence bond theory: Insights from interpretable circuit design," *J. Chem. Theory Comput.* **20**, 3514–3523 (2024).
- ⁸⁹H. G. A. Burton, "Accurate and gate-efficient quantum ansätze for electronic states without adaptive optimization," *Phys. Rev. Res.* **6**, 023300 (2024).
- ⁹⁰H. G. A. Burton, "Tiled unitary product states for strongly correlated Hamiltonians," *Faraday Discuss.* **254**, 157–169 (2024).
- ⁹¹P. A. Johnson, "Beyond a Richardson-Gaudin mean-field: Slater-Condon rules and perturbation theory," *J. Phys. Chem. A* **128**, 6033–6045 (2024).
- ⁹²P. S. Epstein, "The Stark effect from the point of view of Schroedinger's quantum theory," *Phys. Rev.* **28**, 695 (1926).
- ⁹³R. K. Nesbet, "Configuration interaction in orbital theories," *Proc. R. Soc. London, Ser. A* **230**, 312–321 (1955).
- ⁹⁴L. N. Cooper, "Bound electron pairs in a degenerate Fermi gas," *Phys. Rev.* **104**, 1189–1190 (1956).
- ⁹⁵J. Bardeen, L. N. Cooper, and J. R. Schrieffer, "Microscopic theory of superconductivity," *Phys. Rev.* **106**, 162–164 (1957).
- ⁹⁶J. Bardeen, L. N. Cooper, and J. R. Schrieffer, "Theory of superconductivity," *Phys. Rev.* **108**, 1175–1204 (1957).
- ⁹⁷R. W. Richardson, "A restricted class of exact eigenstates of the pairing-force Hamiltonian," *Phys. Lett.* **3**, 277–279 (1963).
- ⁹⁸R. W. Richardson and N. Sherman, "Exact eigenstates of the pairing-force Hamiltonian," *Nucl. Phys.* **52**, 221–238 (1964).
- ⁹⁹R. W. Richardson, "Exact eigenstates of the pairing-force Hamiltonian. II," *J. Math. Phys.* **6**, 1034–1051 (1965).
- ¹⁰⁰M. Gaudin, "Diagonalisation d'une classe d'hamiltoniens de spin," *J. Phys. II* **37**, 1087–1098 (1976).
- ¹⁰¹J.-D. Moisset, C.-É. Fecteau, and P. A. Johnson, "Density matrices of seniority-zero geminal wavefunctions," *J. Chem. Phys.* **156**, 214110 (2022).
- ¹⁰²C.-É. Fecteau, S. Cloutier, J.-D. Moisset, J. Boulay, P. Bultinck, A. Faribault, and P. A. Johnson, "Near-exact treatment of seniority-zero ground and excited states with a Richardson-Gaudin mean-field," *J. Chem. Phys.* **156**, 194103 (2022).
- ¹⁰³P. A. Johnson and A. E. DePrince III, "Single reference treatment of strongly correlated H₄ and H₁₀ isomers with Richardson-Gaudin states," *J. Chem. Theory Comput.* **19**, 8129–8146 (2023).
- ¹⁰⁴P. A. Johnson, "Richardson-Gaudin states," in *Novel Treatments of Strong Correlations, Advances in Quantum Chemistry*, edited by R. A. M. Quintana and J. F. Stanton (Academic Press, 2024), Vol. 90, pp. 67–119.
- ¹⁰⁵The usual definition for PP is less precise: It is a product of pairs, each localized in two orbitals. When optimized for a repulsive interaction, this definition will always reduce to the state defined in Eq. (8).

- ¹⁰⁶M. Piris, X. Lopez, F. Ruipérez, J. M. Matxain, and J. M. Ugalde, "A natural orbital functional for multiconfigurational states," *J. Chem. Phys.* **134**, 164102 (2011).
- ¹⁰⁷K. Pernal, "The equivalence of the Piris Natural Orbital Functional 5 (PNOF5) and the antisymmetrized product of strongly orthogonal geminal theory," *Comput. Theor. Chem.* **1003**, 127–129 (2013).
- ¹⁰⁸S. Jahani, S. Ahmadkhani, K. Boguslawski, and P. Tecmer, "Simple and efficient computational strategies for calculating orbital energies and pair-orbital energies from pCCD-based methods," *J. Chem. Phys.* **162**, 184110 (2025).
- ¹⁰⁹W. Kutzelnigg, "Separation of strong (bond-breaking) from weak (dynamical) correlation," *Chem. Phys.* **401**, 119–124 (2012).
- ¹¹⁰First, the bracketed term under the square root will vanish, leading to a root of 1, and the result of the first summation is 2 times the sum of the orbital energies of the bonding orbitals. In the second term, the occupation numbers will be the integers 1 (bonding) and 0 (anti-bonding) so that only the bonding orbitals contribute. In this limit, the PP state becomes a Slater determinant of fully occupied bonding orbitals.
- ¹¹¹S. Lehtola, J. Parkhill, and M. Head-Gordon, "Orbital optimisation in the perfect pairing hierarchy: Applications to full-valence calculations on linear polyacenes," *Mol. Phys.* **116**, 547–560 (2018).
- ¹¹²M. J. Frisch, M. Head-Gordon, and J. A. Pople, "Semi-direct algorithms for the MP2 energy and gradient," *Chem. Phys. Lett.* **166**, 281–289 (1990).
- ¹¹³W. Kutzelnigg, "Direct determination of natural orbitals and natural expansion coefficients of many-electron wavefunctions. I. Natural orbitals in the geminal product approximation," *J. Chem. Phys.* **40**, 3640–3647 (1964).
- ¹¹⁴M. Hapka, K. Pernal, and H. J. A. Jensen, "An efficient implementation of time-dependent linear-response theory for strongly orthogonal geminal wave function models," *J. Chem. Phys.* **156**, 174102 (2022).
- ¹¹⁵Q. Wang, J. Zou, E. Xu, P. Pulay, and S. Li, "Automatic construction of the initial orbitals for efficient generalized valence bond calculations of large systems," *J. Chem. Theory Comput.* **15**, 141–153 (2019).
- ¹¹⁶J. Zou, K. Niu, H. Ma, S. Li, and W. Fang, "Automatic selection of active orbitals from generalized valence bond orbitals," *J. Phys. Chem. A* **124**, 8321–8329 (2020).
- ¹¹⁷A. Szabo and N. S. Ostlund, *Modern Quantum Chemistry* (McGraw-Hill, New York, 1989).
- ¹¹⁸P. A. Johnson, "Richardson-Gaudin states of non-zero seniority: Matrix elements," *J. Chem. Phys.* **162**, 134106 (2025).
- ¹¹⁹P. A. Johnson, "Richardson-Gaudin states of non-zero seniority. II. Single-reference treatment of strong correlation," *J. Chem. Phys.* **163**, 081101 (2025).
- ¹²⁰M. Piris, "Global method for electron correlation," *Phys. Rev. Lett.* **119**, 063002 (2017).
- ¹²¹I. Mitxelena, M. Rodríguez-Mayorga, and M. Piris, "Phase dilemma in natural orbital functional theory from the N-representability perspective," *Eur. Phys. J. B* **91**, 109 (2018).
- ¹²²M. Rodríguez-Mayorga, P.-F. Loos, F. Bruneval, and L. Visscher, "Time-reversal symmetry in RDMFT and pCCD with complex-valued orbitals," *J. Chem. Phys.* **162**, 054716 (2025).
- ¹²³F. Bruneval, T. Rangel, S. M. Hamed, M. Shao, C. Yang, and J. B. Neaton, "molgw 1: Many-body perturbation theory software for atoms, molecules, and clusters," *Comput. Phys. Commun.* **208**, 149 (2016).
- ¹²⁴M. Rodríguez-Mayorga, Standalone NOFT module (1.0) published on Zenodo (2022).
- ¹²⁵M. Piris and I. Mitxelena, "DoNOF: An open-source implementation of natural-orbital-functional-based methods for quantum chemistry," *Comput. Phys. Commun.* **259**, 107651 (2021).
- ¹²⁶Q. Sun, T. C. Berkelbach, N. S. Blunt, G. H. Booth, S. Guo, Z. Li, J. Liu *et al.*, "PySCF: The Python-based simulations of chemistry framework," *Wiley Interdiscip. Rev.: Comput. Mol. Sci.* **8**, e1340 (2018).
- ¹²⁷P. E. M. Siegbahn, J. Almlöf, A. Heiberg, and B. Roos, "The complete active space SCF (CASSCF) method in a Newton-Raphson formulation with application to the HNO molecule," *J. Chem. Phys.* **74**, 2384–2396 (1981).
- ¹²⁸H.-J. Werner and P. J. Knowles, "A second order multiconfiguration SCF procedure with optimum convergence," *J. Chem. Phys.* **82**, 5053–5063 (1985).
- ¹²⁹Y. Yao and C. J. Umrigar, "Orbital optimization in selected configuration interaction methods," *J. Chem. Theory Comput.* **17**, 4183–4194 (2021).
- ¹³⁰R. Peierls, *Quantum Theory of Solids* (Oxford University Press, London, 1955).
- ¹³¹R. Baxter, *Exactly Solved Models in Statistical Mechanics* (Dover, New York, 2007).
- ¹³²E. T. Jaynes, "Information theory and statistical mechanics," *Phys. Rev.* **106**, 620–630 (1957).
- ¹³³E. T. Jaynes, "Information theory and statistical mechanics. II," *Phys. Rev.* **108**, 171–190 (1957).
- ¹³⁴D. M. Collins, "Entropy maximizations on electron density," *Z. Naturforsch. A* **48**, 68–74 (1993).
- ¹³⁵J. Wang and E. J. Baerends, "Self-consistent-field method for correlated many-electron systems with an entropic cumulant energy," *Phys. Rev. Lett.* **128**, 013001 (2022).
- ¹³⁶A. Y. Zamani and K. Carter-Fenk, "Toward *ab initio* realizations of Collins's conjecture," *J. Chem. Phys.* **163**, 034103 (2025).
- ¹³⁷J. Cioslowski and K. Strasburger, "Constraints upon functionals of the 1-matrix, universal properties of natural orbitals, and the fallacy of the collins "conjecture," *J. Phys. Chem. Lett.* **15**, 1328–1337 (2024).
- ¹³⁸O. Penrose and L. Onsager, "Bose-Einstein condensation and liquid helium," *Phys. Rev.* **104**, 576–584 (1956).
- ¹³⁹C. N. Yang, "Concept of off-diagonal long-range order and the quantum phases of liquid He and of superconductors," *Rev. Mod. Phys.* **34**, 694–704 (1962).
- ¹⁴⁰F. Bloch, "Off-diagonal long-range order and persistent currents in a hollow cylinder," *Phys. Rev.* **137**, A787–A795 (1965).
- ¹⁴¹G.-S. Tian, L.-H. Tang, and Q.-H. Chen, "Pair-mixing superconducting correlation in ultrasmall metallic grains," *Phys. Rev. B* **63**, 054511 (2001).
- ¹⁴²H.-Q. Zhou, J. Links, R. H. McKenzie, and M. D. Gould, "Superconducting correlations in metallic nanoparticles: Exact solution of the BCS model by the algebraic Bethe ansatz," *Phys. Rev. B* **65**, 060502 (2002).
- ¹⁴³A. Faribault, P. Calabrese, and J.-S. Caux, "Exact mesoscopic correlation functions of the Richardson pairing model," *Phys. Rev. B* **77**, 064503 (2008).
- ¹⁴⁴A. Faribault, P. Calabrese, and J.-S. Caux, "Dynamical correlation functions of the mesoscopic pairing model," *Phys. Rev. B* **81**, 174507 (2010).
- ¹⁴⁵D. Hait and M. Head-Gordon, "When is a bond broken? The polarizability perspective," *Angew. Chem.* **135**, e202312078 (2023).
- ¹⁴⁶K. Boguslawski and P. W. Ayers, "Linearized coupled cluster correction on the antisymmetric product of 1-reference orbital geminals," *J. Chem. Theory Comput.* **11**, 5252–5261 (2015).
- ¹⁴⁷K. Boguslawski and P. Tecmer, "Benchmark of dynamic electron correlation models for seniority-zero wave functions and their application to thermochemistry," *J. Chem. Theory Comput.* **13**, 5966–5983 (2017).
- ¹⁴⁸K. Boguslawski, "Open-shell extensions to closed-shell pCCD," *Chem. Commun.* **57**, 12277–12280 (2021).
- ¹⁴⁹S. Lehtola and M. Head-Gordon, "Coupled-cluster pairing models for radicals with strong correlations," *Mol. Phys.* (published online 2025).